Journal of Vertebrate Paleontology 29(1):58–79, March 2009


ARTICLE

# REDESCRIPTION AND PHYLOGENETIC RELATIONSHIPS OF *DOSWELLIA KALTENBACHI* (DIAPSIDA: ARCHOSAURIFORMES) FROM THE UPPER TRIASSIC OF VIRGINIA

DAVID DILKES*[,1] and HANS-DIETER SUES[2]
[1]Department of Biology & Microbiology, University of Wisconsin Oshkosh, Oshkosh, Wisconsin 54901, U.S.A., dilkes@uwosh.edu;
[2]National Museum of Natural History, Smithsonian Institution, MRC 106, P. O. Box 37012, Washington, DC 20013-7012, U.S.A.

ABSTRACT—A detailed redescription of the Late Triassic archosauromorph reptile *Doswellia kaltenbachi* Weems, 1980 from the Poor Farm Member of the Falling Creek Formation in the Taylorsville basin (Newark Supergroup) in Virginia is presented based upon additional preparation of the holotype. The euryapsid skull has a distinctive occiput with a prominent supraoccipital process that is flanked by posterior "horn-like" projections of the squamosals. Postfrontals, tabulars, and postparietals are absent. Plesiomorphic features of the palate and braincase include a plate-like horizontal parabasisphenoid, a pair of foramina for the internal carotid arteries on the ventral surface of the basisphenoid, and two fields of teeth on the palatal surface of the pterygoid. A sharp angle along the cervical and anterior dorsal ribs clearly separates the dorsal and lateral sides of the neck and anterior thoracic region. The posterior thoracic region has shorter ribs that project laterally with only a slight curvature. The ilium has a laterally deflected blade with numerous deep grooves along its distal edge. The laterally extensive set of osteoderms includes a nuchal element that is composed of several interlocking osteoderms that lack the arrangement in distinct transverse rows that characterizes the remainder of the osteoderms. A phylogenetic analysis of basal archosauriforms incorporates new data of *Doswellia* and the taxa *Turfanosuchus*, *Yonghesuchus*, and *Qianosuchus* that have not previously been combined in a single study. Results include a sister-group relationship between *Doswellia* and proterochampsids, placement of *Qianosuchus* as a crurotarsan archosaur, and *Yonghesuchus* and *Turfanosuchus* as successive sister taxa to Archosauria.

## INTRODUCTION

The initial breakup of the supercontinent Pangaea during the Triassic commenced with rifting along the future long axis of the Atlantic Ocean, from Greenland to Mexico (Olsen et al., 1989). This led to the formation of a long chain of rift basins in present-day eastern North America. These basins became filled with thousands of meters of early Mesozoic sediments and, in many cases, basalt flows that are collectively referred to as the Newark Supergroup. Although the sedimentary strata were long considered largely devoid of tetrapod skeletal remains, fieldwork in recent decades, especially in the southern rift basins, has revealed a considerable diversity of Late Triassic amphibians, reptiles, and synapsids.

Among the Triassic tetrapods described to date from the Newark Supergroup, the distinctive, heavily armored reptile *Doswellia kaltenbachi* Weems, 1980 is noteworthy. Although represented by much of the skeleton, the phylogenetic relationships of this taxon have remained uncertain because it combines a considerable number of autapomorphies with plesiomorphic features and most of its appendicular skeleton is still unknown. The type material of *Doswellia kaltenbachi* was collected from siltstones of the Upper Triassic (Carnian) Poor Farm Member or the upper portion of the Falling Creek Formation (Doswell Group) in the Taylorsville basin of the Newark Supergroup in eastern Virginia (LeTourneau, 2003). The Poor Farm Member comprises gray, gray-green, dark gray, and black sandstone, siltstone, calcareous sandstone and siltstone, and thin coaly layers (LeTourneau, 2003). Its dark-gray and black siltstones have yielded well-preserved remains of a diverse flora (Cornet and Olsen, 1990), abundant casts of unionid shells, and isolated fish scales. To date, tetrapods are represented only by unidentified archosaurian teeth and *Doswellia* (Weems, 1980).

Based on palynological data, Cornet and Olsen (1990) argued for a Carnian age for the fluviolacustrine Taylorsville basin sequence 1 (TVB1), which includes the unit from which *Doswellia* is known. Huber et al. (1993) and Lucas and Huber (2003) assigned *Doswellia* to their Sanfordian Land Vertebrate Faunachron (LVF) for eastern North America. Huber et al. (1993) considered the Sanfordian LVF late Carnian (Tuvalian) in age, but Lucas and Hunt (2003) extended the possible age range for this faunachron to ?early to late Carnian (Julian to early Tuvalian) and dated the Falling Creek Formation as ?Julian.

Long and Murry (1995) described and illustrated a number of vertebrae and osteoderms as well as what appears to be a disarticulated carapace from the Dockum Group of Howard County, Texas, and referred them to *Doswellia kaltenbachi*. This referral appears justified because the Texas and Virginia specimens share features such as a large articular facet and a dorsal eminence with many small pits on each osteoderm and elongated, ventrally concave diapophyses on the dorsal vertebrae. To date, the remains from the Dockum Group represent the only known record of *Doswellia* outside the Taylorsville basin.

Additional preparation of the material of *Doswellia kaltenbachi* described by Weems (1980) has revealed new anatomical features of this distinctive reptile. In this paper we redescribe *Doswellia* in detail and provide a revised diagnosis. We also present a new phylogenetic analysis to assess the phylogenetic position of *Doswellia* among basal archosauriforms and to test current hypotheses of archosauriform interrelationships.

**Institutional Abbreviations—USNM**, National Museum of Natural History (formerly United States National Museum), Smithsonian Institution, Washington, DC.

**Anatomical Abbreviations—ac**, rim for articular capsule of joint; **af**, articular facet; **an**, angular; **ap**, anterior projection; **ar**,

*Corresponding author.

articular; **ax**, axis; **bo**, basioccipital; **bpt**, basipterygoid process; **bt**, basal tuber of basioccipital; **cap**, capitulum; **cpr**, cultriform process; **de**, dorsal eminence; **df**, distal facet; **dia**, diapophysis; **ec**, ectopterygoid; **eo**, exoccipital; **f**, frontal; **fc**, rim for fibrous capsule of joint; **for**, foramen; **ica**, foramen for cerebral branch of internal carotid artery; **i. tub.**, ischial tuberosity; **j**, jugal; **mf**, metotic foramen; **mx**, maxilla; **of**, obturator foramen; **op**, opisthotic; **or. marg.**, orbital margin; **p**, parietal; **pbs**, parabasisphenoid; **pal**, palatine; **para**, parapophysis; **po**, postorbital; **pt**, pterygoid; **p. tub.**, pubic tuberosity; **q**, quadrate; **qj**, quadratojugal; **rtp**, retroarticular process; **sa**, surangular; **so**, supraoccipital; **sq**, squamosal; **st.f.**, supratemporal fenestra; **su.an.**, suture for angular; **su.ar.**, suture for articular; **su.d.**, suture for dentary; **su. ec.**, suture for ectopterygoid; **su.l.**, suture for lacrimal; **su.m.**, suture for maxilla; **su.po.**, suture for postorbital; **su.pra.**, suture for prearticular; **su.qj.**, suture for quadratojugal; **su.sa.**, suture for surangular; **su.sq.**, suture for squamosal; **tp**, tooth puncture; **tub**, tuberculum; **vrop**, ventral ramus of opisthotic; **vt**, crista ventrolateralis; **XII**, foramen for N. hypoglossus (XII).

## SYSTEMATIC PALEONTOLOGY

DIAPSIDA Osborn, 1903
ARCHOSAUROMORPHA Huene, 1946
DOSWELLIIDAE Weems, 1980
*DOSWELLIA KALTENBACHI* Weems, 1980
(Figs. 1–15)

**Holotype**—USNM 244214, "axial skeleton from seventh cervical through fifth caudal, scattered more posterior caudals, associated ribs; pelvis complete except for left ischium; clavicle, interclavicle; dorsal and lateral armor badly shattered except for an articulated patch from the posterior region" (Weems, 1980:12).

The paratype designated by Weems (1980), USNM 214823, comes from the same locality and bedding plane and probably belongs to the same individual as the holotype. However, this association could not be definitely established. It comprises the postorbital portion of the skull, postdentary bones of the mandible, second through fifth cervicals, cervical ribs, nuchal armor, cervical osteoderms, and the distal end of a ?tibia (Weems, 1980:12). An isolated right jugal, USNM 437574, was also recovered from the locality, indicating the presence of at least two individuals.

**Horizon and Locality**—Poor Farm Member of the Falling Creek Formation (Doswell Group; LeTourneau, 2003), Taylorsville basin. Age: Late Triassic (Carnian). Pit dug for foundation of Doswell sewer plant, 0.4 miles (0.64 km) northwest of the confluence of the North Anna River and the Little River, near Doswell, Hanover County, Virginia, U.S.A.

**Referred Specimens from the Taylorsville Basin**—USNM 25840, cervical vertebra, dorsal vertebra, bone fragments. Near Ashland, Hanover County, along Richmond, Fredericksburg and Potomac Railway right-of-way, about 1.5 miles (2.4 km) north of Route 54, Virginia, U.S.A. USNM 186989, left dentary, cervical vertebra, posterior dorsal vertebra, left femur, disassociated osteoderms. USNM 244215, centrum of anterior dorsal vertebra. Both from northeast streambank of creek on east side of Richmond, Fredericksburg and Potomac Railway, 1.2 miles (1.92 km) north of Ashland, Hanover County, Virginia, U.S.A.

**Revised Diagnosis**—Archosauromorph diapsid characterized by the following autapomorphies: elongate diapophyses of dorsal vertebrae with ventral concave and rugose surfaces for articulation with elongate capitulum of dorsal ribs; sharply angled cervical and anterior dorsal ribs; abrupt change in cross-sectional shape of rib cage from narrow to wide between anterior and posterior dorsal vertebrae; extensive series of osteoderms forming transverse rows from back of skull to at least base of tail and including at least five longitudinal rows on each side of vertebral column in posterior dorsal region; ilium with laterally deflected dorsal blade. *Doswellia* is also distinguished by the following unique combination of features: prominent occipital peg of supraoccipital that projects over dorsal rim of foramen magnum; euryapsid construction of temporal region with enlarged jugal below supratemporal fenestra; absence of postparietals, tabulars, and postfrontals; small elliptical supratemporal fenestra that does not reach occipital margin; squamosals with posteriorly directed "horn-like" processes; elongate convex dorsal end of quadrate that fits into elongate ventral groove on squamosal; step between the flat skull roof and temporal region; absence of lateral mandibular fenestra; teeth with slender, conical crowns lacking carinae; three sacral ribs, the first derived from dorsal region; pair of oval articular facets at distal tips of first two caudal ribs.

## DESCRIPTION

### Skull

The known cranial remains of *Doswellia* consist of the postorbital portion of a skull associated with a left angular, both surangulars, and a right articular (USNM 214823) and an isolated right jugal (USNM 437574) from the Doswell locality. Weems (1980) reconstructed a long and tapering rostrum for *Doswellia* based on a referred left dentary (USNM 186989) from the Ashland locality. The dentary was found with isolated vertebrae and osteoderms that conform to those of the holotype of *Doswellia kaltenbachi*, and the teeth preserved in alveoli 3 and 4 closely resemble a tooth in the left maxilla of USNM 214823 in the possession of slender, conical crowns without carinae.

As preserved, the postorbital region of USNM 214823 is broad and dorsoventrally flattened largely as a result of crushing during fossilization (Fig. 1). Nevertheless, once this distortion is corrected, the width of the skull is clearly several times its height. On each side of the temporal region, there is only a single temporal fenestra, which is bounded by the parietal medially, the postorbital and squamosal laterally, and the squamosal posteriorly (Fig. 1A). This opening is evidently an upper temporal (supratemporal) fenestra, and the temporal configuration could thus be described as euryapsid. Only two other euryapsid archosauromorph reptiles are known from the Late Triassic: *Trilophosaurus* Case, 1928 from the Dockum Group (Carnian-Norian) of Texas and the Chinle Formation of Arizona (Gregory, 1945; Long and Murry, 1995; Heckert et al., 2006; Mueller and Parker, 2006) and *Teraterpeton* Sues, 2003 from the Wolfville Formation (Carnian) of the Fundy basin (Newark Supergroup) in Nova Scotia. Unlike the large temporal openings of *Trilophosaurus* and *Teraterpeton*, the supratemporal fenestrae of *Doswellia* are small and do not extend posteriorly beyond the occipital condyles. The posteriorly enlarged temporal fenestrae of *Trilophosaurus* and *Teraterpeton* create deeply embayed occipital margins. The occipital margin of *Doswellia* is also embayed, but this is due to the presence of posterior, "horn-like" extensions of the squamosals. Furthermore, rather than having a single embayment between the right and left squamosals, the occipital embayment of the skull of *Doswellia* is divided into two regions by a posterior "spur-like" extension of the parietals along their median suture and the dorsal exposure of the supraoccipital. In addition to the embayment of the occipital margin, the posterior edge of the squamosal lateral to its "horn-like" extensions is curved anteriorly and joins a similar curvature of the quadratojugal. Postparietals, tabulars and supratemporals that would be present along the occipital region of a more basal diapsid are absent in *Doswellia*. Weems's (1980:fig. 8) reconstruction of the skull shows the quadrate in line with the occipital condyle. However, the quadrates have been displaced anteriorly and laterally by postmortem crushing, and, once

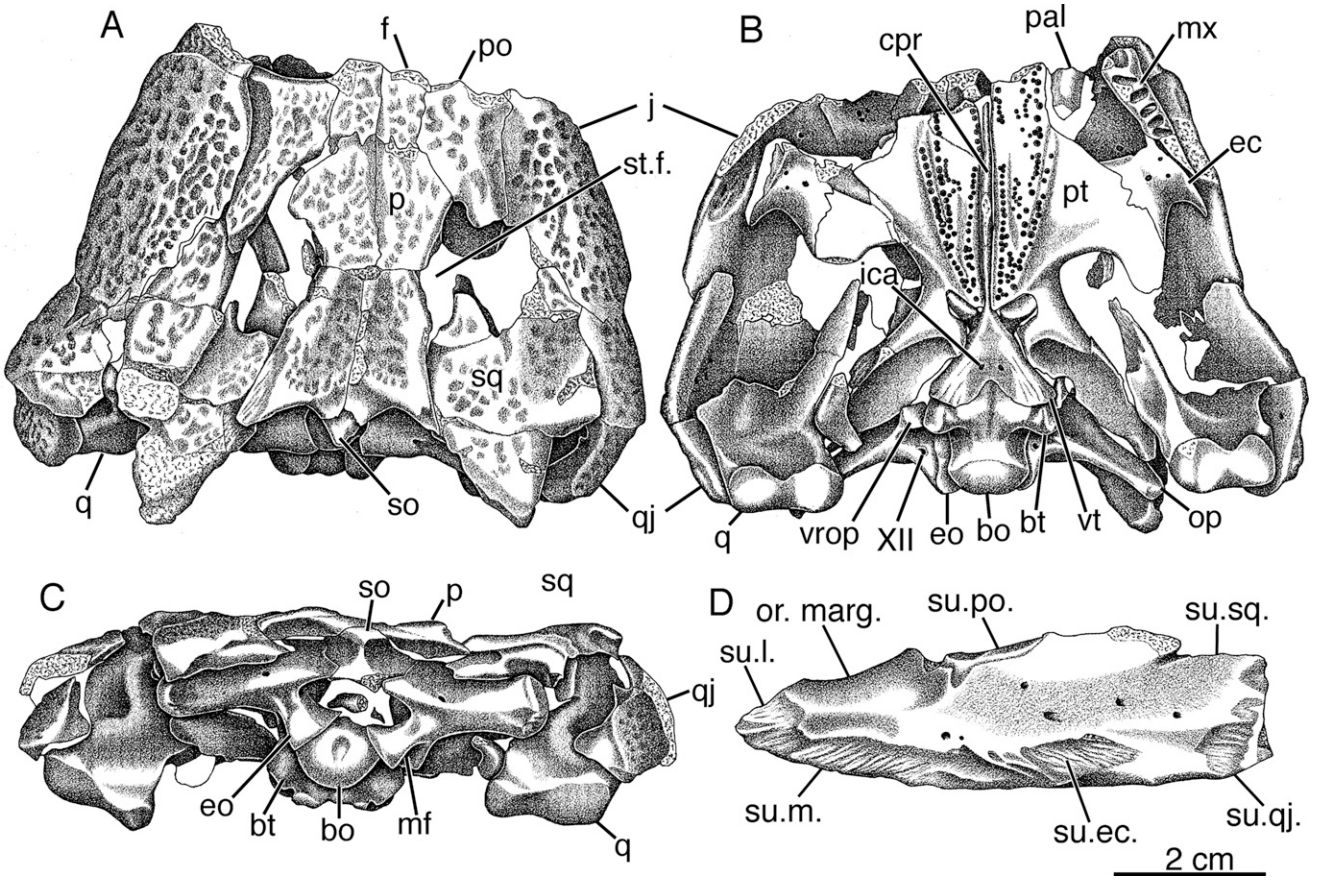


FIGURE 1. Skull of *Doswellia kaltenbachi*. **A–C**, postorbital region (USNM 214823) in dorsal (**A)**, ventral (**B)**, and occipital views (**C)**; **D**, isolated right jugal (USNM 437574) in medial view.

placed in their correct articulation with the pterygoids, would extend posterior to the occipital condyle.

The skull table, which is formed by the posterior ends of the frontals, the parietals, and most of the postorbitals and squamosals, is flat and horizontal. A "step" between the skull table and the convex lateral side of the temporal region extends along the postorbital and squamosal between the orbit and the posterior edge of the skull just lateral to the "horn-like" extensions of the squamosal. This step is probably not as pronounced as restored by Weems (1980:fig. 8). It does not enter the orbit nor does it reach the posterior edge of the squamosal.

The preserved section of the palate is essentially horizontal (Fig. 1B). Although incomplete due to the absence of the antorbital region in USNM 214823, the suborbital fenestra was clearly quite large and bordered by the palatine, pterygoid, ectopterygoid and maxilla.

The external surfaces of the dermal bones of the skull bear deeply incised pits that vary from oval to circular in outline. There appears to be little pattern to the arrangement of these pits although those near the edges of a bone are frequently more elongate than those closer to the center of the bone.

### Dermal Bones of the Skull

Only the jugals, postorbitals, frontals, parietals, squamosals, quadratojugals, pterygoids, ectopterygoids and small portions of the left palatine and maxilla are preserved in the skull of USNM 214823. Both jugals of this specimen lack the suborbital ramus. An isolated right jugal (USNM 437574; Fig. 1D), only slightly damaged along its posterior edge, reveals details of its medial surface not readily visible in USNM 214823. The jugal is a long bone with a length that is over three times its height. It forms a significant portion of the temporal region and curves dorsally onto the skull table, evidently occupying much of the area of the cheek that bears the infratemporal fenestra of a typical diapsid reptile. Anteriorly, the jugal forms most of the ventral and a small portion of the posterior rim of the orbit. A long sutural surface along its ventral edge for the maxilla extends from the midpoint of the bone anteriorly onto its bluntly pointed anterior end. As there is a considerable region of bone between the dorsal extent of the maxillary suture and the orbital rim, it is unlikely that the maxilla contributed to the orbital margin. Immediately posterior to the suture with the maxilla is a rhomboidal sutural facet for the ectopterygoid. Above the contact with the ectopterygoid, a largely horizontal sutural facet for the postorbital extends from the orbital rim to the midpoint of the jugal. The remainder of the dorsal edge of the jugal is a sutural surface for the squamosal. The damaged posterior end of the jugal contacted the quadratojugal. Only the posterior tip of the left maxilla is preserved. Six alveoli are present. A partial tooth, preserved in the fourth preserved alveolus, establishes that the crown was slender, smooth, and recurved.

The bone interpreted as the postorbital by Weems (1980) and the present authors is a narrow, triangular element. The base of this bone forms most of the posterior rim of the orbit. Its elongate, posterior ramus narrows to a blunt point and has an extensive lateral contact with the jugal, more restricted contacts medially with the frontal and parietal, and overlaps the inner

side of the anterior process of the squamosal. Together with the squamosal, the postorbital forms the lateral rim of the supratemporal fenestra.

Only a small, posterior portion of each frontal is preserved in the paratype. The suture with the postorbital is at a right angle to the interdigitated, transverse contact between the frontal and parietal. The left frontal preserves a small portion of the posterior orbital rim. The parietals form the transversely gently concave central portion of the skull deck, with a shallow depression along the midline suture that extends from the midpoint of the supratemporal fenestrae to near the occipital margin. The lateral edges of the parietals are embayed slightly to form the medial rims of the supratemporal fenestrae. The occipital margin of the parietals is expanded and embayed with the midline extended posteriorly and a small dorsal exposure of the supraoccipital to create a bluntly pointed projection. The posterior extension of the parietals and the exposure of the supraoccipital are recessed below the surface of the skull table.

The large squamosal forms the posterior edge and about half the lateral edge of the temporal fenestra. Medially, it has a long butt suture with the parietal from the supratemporal fenestra to the occipital margin. A part of this medial region is drawn out posteriorly to form the "horn-like" process. Along the occiput, the medial region contacts the paroccipital process of the opisthotic. There are similar contacts between the parietal and paroccipital process and supraoccipital that completely cover the region where a posttemporal fenestra would be otherwise present. A broad ventral portion of the squamosal extends from the step between the dorsal and lateral sides of the skull to contact the quadratojugal and jugal. This ventral portion also extends anteriorly to contact the postorbital. The quadrate fits into a recess along the occipital margin of the squamosal in a fashion similar to other archosauromorphs. However, rather than the dorsal part of the quadrate forming a ball that fits into a socket-like depression on the squamosal, the quadrate of *Doswellia* has an elongated, convex, and posteriorly directed process that fits into a long groove on the ventral surface of the squamosal. The quadratojugal at the posterior corner of the skull contacts the jugal anteriorly, the squamosal dorsally, and the quadrate posteriorly. The contact between the quadratojugal and quadrate includes a smooth, tapering process that overlaps the occipital face of the quadrate. The deeply curved posterior edge of the quadratojugal extends anteriorly as least to the same level as the occipital curvature of the parietals.

The plate-like pterygoids dominate the palatal surface (Fig. 1B). A narrow interpterygoid vacuity divided by the cultriform process separates the pterygoids along the midline. The pterygoids have several anteroposterior fields of teeth on raised bone ridges separated by grooves. One field is a single row of teeth next to the interpterygoid vacuity that extends from the basipterygoid articulation to the preserved anterior end of the pterygoid. This row of teeth corresponds topographically to the third field of teeth described in *Mesosuchus* (Dilkes, 1998) and present in other archosauromorphs such as *Prolacerta* (Modesto and Sues, 2004:fig. 6B) and *Proterosuchus* (Welman, 1998:fig. 1, "T3"). It is a continuation of a single row of medially curved teeth along the edge of the interpterygoid vacuity in *Mesosuchus* (Dilkes, 1998) and *Prolacerta*. A similar row of teeth is found along the entire medial edge of the pterygoid of *Proterosuchus* (Welman, 1998:fig. 1, "T4"). These medially curved teeth are absent in *Doswellia*. A second field of palatal teeth in *Doswellia* extends across the pterygoid from the basicranial articulation towards the palatine. A comparable field of teeth is also present in *Euparkeria* (Ewer, 1965), *Mesosuchus* (Dilkes, 1998), *Prolacerta* (Modesto and Sues, 2004), and *Proterosuchus* (Welman, 1998:fig. 1, "T2"). The lateral part of the transverse flange along the contact with the ectopterygoid extends posteriorly into the adductor chamber as a large, rounded projection. The transverse flange is devoid of teeth. Each basipterygoid process fits into a deep and narrow recess that is accentuated by a pronounced medial projection of the quadrate ramus of the pterygoid that nearly reaches the parasphenoid. The remainder of the quadrate ramus consists of a deep, medially concave and vertical flange. At the junction between this vertical flange and the medial projection posterior to the basipterygoid process, the quadrate process has a deep, cup-shaped depression.

The ectopterygoid forms extensive, broad contacts with the lateral edge of the pterygoid and medial edges of the maxilla and jugal. Along the anterior half of the interdigitating ectopterygoid-pterygoid suture, the pterygoid overlaps the ventral surface of the ectopterygoid as in many archosauromorphs (Dilkes, 1998). The posterior half forms a butt suture. Three small foramina are present on the ventral surface of each ectopterygoid. Only a small posterior portion of the palatine is preserved along the lateral margin of the pterygoid. A pronounced ridge lacking any evidence of teeth would align with the raised denticulated area of the pterygoid that extends across the palatal surface from the basipterygoid articulation to the palatine.

The quadrate is a robust bone. As noted above, both elements are complete but displaced anteriorly as well as laterally away from their original positions. The posterior surface of the quadrate is concave, but not nearly to the same degree as in other archosauromorphs such as *Mesosuchus* (Dilkes, 1998), *Prolacerta* (Modesto and Sues, 2004), *Proterosuchus* (Welman, 1998), and *Teraterpeton* (Sues, 2003). The curvature of the quadrate of *Doswellia* is pronounced, as noted by Weems (1980), by the unusually recurved proximal process that fits into an elongate recess of the squamosal. The recurved proximal end and the posterior edge of the more distal portion of the quadrate enclose between them a distinct notch. The edge of this process continues ventrally along the posterior surface of the quadrate to the midpoint of the bone and then curves laterally towards the overlapping, tapering process of the quadratojugal. A deep pocket is developed at the confluence of the vertical and horizontal segments of this edge. No quadrate foramen is present. A large, tapering medial flange of the quadrate overlaps the lateral surface of the quadrate ramus of the pterygoid. The paired, rounded condyles at the distal end of each quadrate are approximately equal in size. The quadrates are inclined medially when moved back to their natural position. A portion of the columella of the right epipterygoid is visible in oblique ventrolateral view.

**Braincase**

The basioccipital forms most of the occipital condyle, with the exoccipitals contributing only the dorsolateral corners of the condyle. A distinct notochordal pit is present on its posterior surface. The exoccipitals do not meet along the dorsal surface of the condyle, and the basioccipital makes a small contribution to the ventral margin of the foramen magnum. Immediately anterior to the occipital condyle, the basioccipital narrows to a distinctive neck similar to that seen in *Erythrosuchus* (Gower, 1997). Further anteriorly, the lateral edges of the basioccipital form a pair of large, ventrolaterally projecting basal tubera. The flattened distal end of each tuber is overlapped slightly by the fused parabasisphenoid. A prominent groove on the ventral surface of the basioccipital begins on the neck and continues anteriorly to the contact with the parasphenoid where it merges with a broader depression on the basioccipital and basisphenoid. This latter depression, noted in other archosauromorphs, is referred to as the basioccipital-basisphenoid fossa (Gower and Sennikov, 1996; Gower and Weber, 1998).

Each exoccipital has an expanded base along the dorsal and lateral surfaces of the occipital condyle that narrows before

fusing indistinguishably with the opisthotic. The exoccipital forms the posterior wall of the metotic foramen for cranial nerves IX to XI (Nn. glossopharyngeus, vagus, and accessorius) and the internal jugular vein. On the lateral surface of the narrow region of the exoccipital just posterior to the metotic foramen is a prominent foramen that was the exit for passage of cranial nerve XII (N. hypoglossus). The anterior extent of the base of the exoccipital, revealed on the displaced right exoccipital, shows that the exoccipital reached towards, but apparently did not contact the ventral ramus of the opisthotic. Thus, there appears to be only a small contribution of the basioccipital to the floor of the metotic foramen. There is no contact between the exoccipital and either the basisphenoid or prootic. No facet for the proatlas is visible on either exoccipital. Dorsally, the exoccipitals are separated by the supraoccipital, which forms the dorsal margin of the foramen magnum.

The opisthotic bears a ridge that reaches from its contact with the supraoccipital to close to the distal end of the paroccipital process. The slightly expanded distal end of the paroccipital process is rounded anteroposteriorly and strongly curved dorsoventrally. The distal end of each paroccipital process has a flattened lateral edge suggestive of contact with the quadrate. A shallow concavity on the occipital portion of the squamosal receives the distal end of the paroccipital process. The remainder of the occipital exposure of the squamosal overlaps the opisthotic, and there is no posttemporal fenestra. Nutrient blood vessels and small nerves most likely passed through a small foramen on the occipital side of each paroccipital process. The structure of the ventral ramus of the opisthotic that separates the metotic foramen and fenestra ovalis is shown by the displaced right opisthotic. Dorsally, this ramus forms a thin blade, but it expands greatly ventrally to a large rectangular foot that contacts the basioccipital. Opisthotics of other archosauromorphs such as *Mesosuchus* (Dilkes, 1998), *Prolacerta* (Evans, 1986), *Euparkeria* (Gower and Weber, 1998), and erythrosuchids and proterosuchids (Gower, 1997; Gower and Sennikov, 1996, 1997) have similar, although in some instances less prominent, distal expansions. Given the close fit between the ventral ramus of the opisthotic and the cristae ventrolaterales and basal tubera of the basioccipital, any "pseudolagenar recess" (Gower and Sennikov, 1996, 1997), if present, would be very small.

Anterior to the opisthotic, the prootic forms most of the sidewall of the braincase. A small, exposed portion of the right prootic includes the posteroventral margin of the notch for N. trigeminus (V).

The basisphenoid and parasphenoid are indistinguishably fused. Accordingly, the combined unit will be referred to as the parabasisphenoid. The parabasisphenoid of *Doswellia* retains the horizontal, plate-like configuration found in other archosauromorphs such as *Prolacerta* (Evans, 1986), *Proterosuchus* (Cruickshank, 1972), and *Fugusuchus* (Gower and Sennikov, 1996). *Mesosuchus* also has a plate-like parabasisphenoid, but it is not positioned horizontally (Dilkes, 1998). There is no intertuberal plate on the basisphenoid. The cristae ventrolaterales (also referred to as the basal tubera of the basisphenoid) bear several deep grooves and are separated by the basioccipital-basisphenoid fossa. At the base of the cristae ventrolaterales and within the approximate anterior limit of the basioccipital-basisphenoid fossa is a pair of foramina for the cerebral branches of the internal carotid arteries. No vidian canals or other surface features are present to indicate the likely courses of the palatine branches of N. facialis (VII) and the internal carotid arteries. The large basipterygoid processes project anterolaterally at approximately 45° to the midline. Each process has an elongated articular surface on its anterior surface for the pterygoid. Displacement of the quadrate rami of the pterygoids obscures the sides of the parabasisphenoid so it is uncertain if a semilunar depression (Gower, 1997; Gower and Sennikov, 1996) is present on the basisphenoid. The cultriform process of the parasphenoid is exposed between the palatal rami of the pterygoids; it is not clear whether this exposure is due to the dorsoventral crushing of the skull. Its anterior end is incomplete. A small piece of bone on the right side of the braincase is possibly a portion of the laterosphenoid.

The supraoccipital bears a median ridge that begins on the shelf-like portion of the bone above the foramen magnum and merges with a prominent, triangular occipital projection of the parietals. No sculpturing is present on the supraoccipital.

There is a nearly complete left stapes and the distal end of the right stapes. The stapedial shaft is slender and rod-like, terminating laterally in the notch formed by the recurved proximal head of the quadrate.

**Mandible**

The type material of *Doswellia kaltenbachi* preserves only isolated elements of the posterior region of the lower jaw. Enough is preserved, however, to establish the absence of a lateral mandibular fenestra.

The right and left surangulars, right angular, and right articular are preserved in the paratype of *Doswellia kaltenbachi* (Fig. 2A–H). The dorsal edge of the surangular along the rim of the adductor fossa is thin and gently convex. It lies above a strong ridge on the medial surface that extends from the suture with the dentary to the complex facets for the articular. A long, broad groove extends anteriorly from a large foramen along the ventral side of the ridge and continues anteriorly beneath the suture for the dentary. A smoothly concave region immediately lateral and anterior to the complex sutures for the articular represents the contribution of the surangular to the lateral portion of the mandibular facet of the jaw joint. There are no anterior or posterior surangular foramina on the lateral surface of the surangular, unlike the condition in archosauromorphs such as *Euparkeria* (Ewer, 1965), *Prolacerta* (Modesto and Sues, 2004), and *Proterosuchus* (Welman, 1998). A posterior extension of the surangular covers most of the lateral surface of the articular almost to the posterior end of the retroarticular process that extends well below the level of the jaw joint. The surangular overlaps the angular laterally, forming is a relatively straight, horizontal suture. This overlap is quite extensive beneath the jaw joint, but is much more restricted anteriorly.

The angular bears only light sculpturing on its lateral side and probably contacted the retroarticular process. Its anterior extent is unknown, but reached at least to the posterior limit of the suture between the surangular and dentary.

The articular forms the medial portion of the mandibular facet of the jaw joint. Its deep, subrectangular retroarticular process projects ventromedially below the level of the facet for the jaw joint. Only a small part of this process would be visible in lateral view posterior to the surangular and angular when the jaw elements are reassembled.

The isolated left dentary (USNM 186989; Fig. 2I–K) referred to *Doswellia* by Weems (1980) is very long, low, and strongly concave laterally. The element was considerably damaged during the original preparation. The mandibular symphysis apparently extends back to the level of the tenth or eleventh alveolus. There are only a few pits on the lateral side along the alveolar margin and near the anterior end of the bone. Alveoli for 35 teeth are present; the individual sockets are separated by well-developed bony septa, and a narrow groove extends lingual to the alveoli. Tooth implantation is thecodont. The posterior six alveoli appear to be smaller than the preceding ones. The third dentary alveolus contains the apical portion of an erupting tooth, and the base of a broken tooth is preserved in the fourth alveolus from the tip. Together, these teeth indicate that the tooth crowns were slender, conical, and gently recurved.

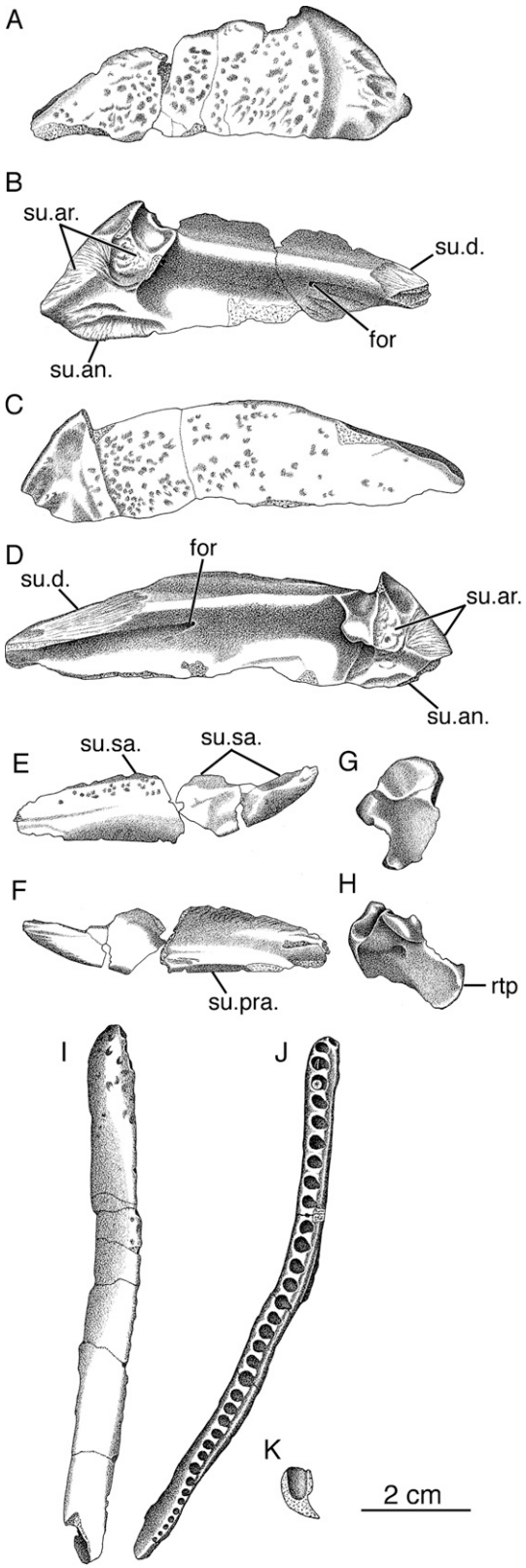


FIGURE 2. Mandible of *Doswellia kaltenbachi*. **A**, **B**, left surangular (USNM 214823) in lateral (**A**) and medial (**B**) views; **C, D**, right surangular (USNM 214823) in lateral (**C**) and medial (**D**) views; **E**, **F**, left angular (USNM 214823) in lateral (**E**) and medial (**F**) views; **G**, **H**, right articular (USNM 214823) in dorsal (**G**) and medial (**H**) views; **I–K**, referred partial left dentary (USNM 186989) in lateral (**I**) and dorsal (**J**) views, with **K**, a transverse section at the level of alveolus 15.

**Postcranial Axial Skeleton**

Cervical, anterior dorsal, sacral, and caudal vertebrae are disarticulated, but remain associated within each region. Only the posterior dorsals are articulated or only slightly separated. All ribs are disarticulated, but do not appear to have been greatly displaced. Ribs in the posterior dorsal region can be confidently associated with a specific vertebra. Twenty-two presacrals, three sacrals, and 13 caudals are preserved (Weems, 1980). An open suture is visible between the neural arch and centrum of the cervicals, dorsals, sacrals, and first five caudals, demonstrating that this individual was not skeletally mature.

**Cervical Vertebrae**—Only a few cervical vertebrae are complete. Weems (1980) estimated a count of eight cervical vertebrae based upon the presence of cervical ribs next to these vertebrae. However, the exact location of the cervical-dorsal transition is uncertain because no ribs are associated with the incomplete ninth vertebra. The neural spine of the axis is low with a sharp dorsal edge (Fig. 3A, B). The posterior zygapophyses are strongly angled and separated by a deep concavity. The anterior edges of the neural arch that rise above each posterior zygapophysis are crenulated, probably indicating the presence of an interlaminar elastic ligament that extended between neighboring vertebrae as in crocodylians (Frey, 1988). The presence of an anterior protuberance (Weems, 1980) cannot be confirmed because the axial neural arch and spine are broken.

Each postaxial cervical vertebra has a tall and narrow neural arch that is pinched in the middle (Fig. 3C, D). The large neural canal is wider than tall beneath the prezygapophyses and taller than wide beneath the postzygapophyses. A ridge extends across the side of the neural arch connecting the pre- and postzygapophyses and a second ridge connects the postzygapophysis and diapophysis. A third ridge extends from the diapophysis to the posterior edge of the centrum. The zygapophyses are elevated above the centrum and their facets are angled along the transverse plane at least 40° and the parasagittal plane at approximately 30°. The neural spine is tall with a much shorter anteroposterior length than on the axis. The neural spine is narrowest along the anterior edge and widens posteriorly approximately 3.5 times. The dorsal edge and upper portion of the posterior edge of the neural spine is slightly roughened with a distinct lip separating the two surfaces. This roughened surface is the probable attachment site for supraspinal ligaments and ligaments joining the paramedian osteoderms to the vertebrae. The amphicoelous centrum is constricted in its middle, and has a low ridge along its ventral surface. The articular surfaces of the centrum are horizontally oval. A deep groove separates the prominent diapophysis and the shorter parapophysis both of which are directed ventrolaterally.

**Anterior Dorsal Vertebrae**—Anterior (Fig. 4A–C) and posterior (Fig. 4D–F) dorsals can be distinguished based on differences in the shapes of the vertebrae and their ribs. The first five are anterior dorsals and the remaining eight are posterior dorsals. The diapophysis of the anterior dorsals becomes progressively larger toward the posterior end of the series and, at least on the last three of the sequence, projects laterally and slightly posteriorly. In contrast, the parapophysis becomes smaller until it forms little more than a slightly raised, flattened surface beneath the diapophysis. Whereas the articular surfaces for the cervical ribs are restricted to the distal ends of the dia- and parapophyses, the ventral surface of the lengthened diapophysis on the anterior dorsals is an additional articular surface for the capitulum of the dorsal rib (Fig. 4B). This type of rib articulation is unique to *Doswellia*. The ventral articular surface of the diapophysis becomes increasingly rugose and concave to provide a firmer connection with the rib. The tuberculum articulates with the distal end of the diapophysis as in the cervicals. An additional feature of the diapophysis of anterior dorsals is a flange-like

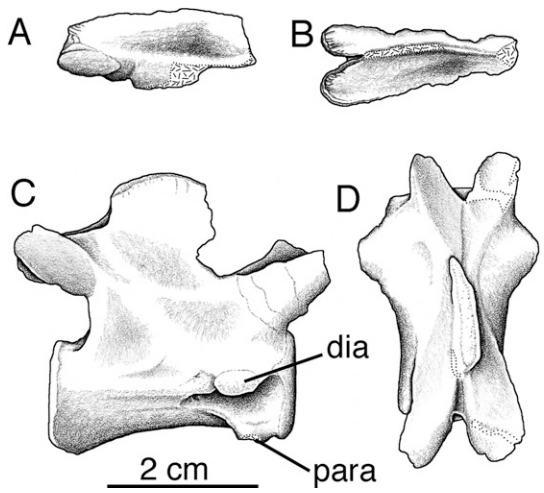


FIGURE 3. Cervical vertebrae of *Doswellia kaltenbachi*. **A**, **B**, axis (USNM 214823) in right lateral (**A**) and medial (**B**) views; **C**, **D**, seventh cervical vertebra (USNM 244214) in right lateral (**C**) and dorsal (**D**) views.

process along the anterior margin. The ventral surface of this anterior process is rugose, but clearly set apart from the rugose ventral region for the capitulum. The zygapophyseal articular facets for the first pair of anterior dorsals, though distorted and damaged, differ little in their orientation from those of the last cervicals. However, these facets are virtually horizontal. Neural spines continue to have a thin anterior edge, but otherwise are much wider than on the cervicals. The dorsal surface of the neural spine is slightly roughened and bulbous. Numerous fine ridges extend down the side of the neural spine from the dorsal tip. The centrum is cylindrical with very little or no constriction. Its ends are amphicoelous, with an oval outline similar to that of the cervical centra.

**Posterior Dorsal Vertebrae**—The diapophysis attains its maximum length in the first pair of posterior dorsals and decreases thereafter. The entire ventral surface of the diapophysis, which is more dorsally concave than in the anterior dorsals (Fig. 4E), articulates with the dorsal edge of the capitulum. There is no longer any discernible parapophysis. Instead, the end of the capitulum inserts into a concavity ventral to the base of the diapophysis. An oval articular facet for the tuberculum is present at the distal tip of all diapophyses except those of the last dorsal where the distal ends are blade-like. An anterior flange on the diapophysis of the anterior dorsals is absent. The centrum is amphicoelous and constricted in the middle. The orientation of the zygapophyses remains horizontal as in the anterior dorsals with the exception of the last two that show a medial inclination. The structure of the neural arch and neural spine differs little from that of the anterior dorsals.

**Sacral Vertebrae**—There is a striking structural difference between the anterior and posterior halves of the first sacral vertebra (Fig. 5A, B), indicating that this vertebra is a dorsal that became incorporated into the sacrum (Weems, 1980). The diapophysis is similar to that of the last dorsal though much shorter, the shape and orientation of the prezygapophysis matches the last dorsals, and the anterior face of the centrum is oval. The parapophysis is, however, clearly differentiated. In the posterior half, the postzygapophyses are much closer to the midline with smaller, more elongate facets, and the centrum is much lower and expanded laterally to support the large articular surfaces for the second sacral rib. The neural spines of the sacrals are bulbous with fine ridges. The three sacral vertebrae form a

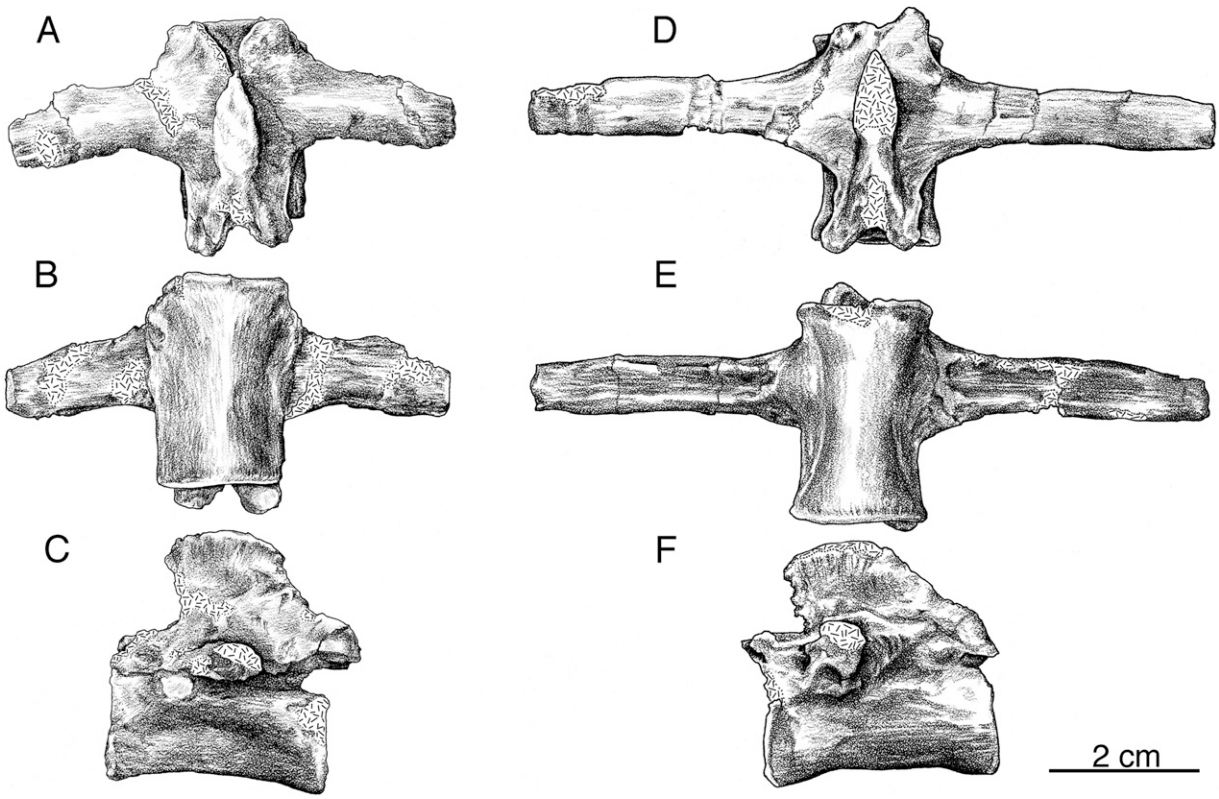


FIGURE 4. Dorsal vertebrae of *Doswellia kaltenbachi* (USNM 244214). **A**–**C**, fourth dorsal vertebra in dorsal (**A**), ventral (**B**), and left lateral (**C**) views; **C**-**F**, seventh dorsal vertebra in dorsal (**D**), ventral (**E**), and left lateral (**F**) views.

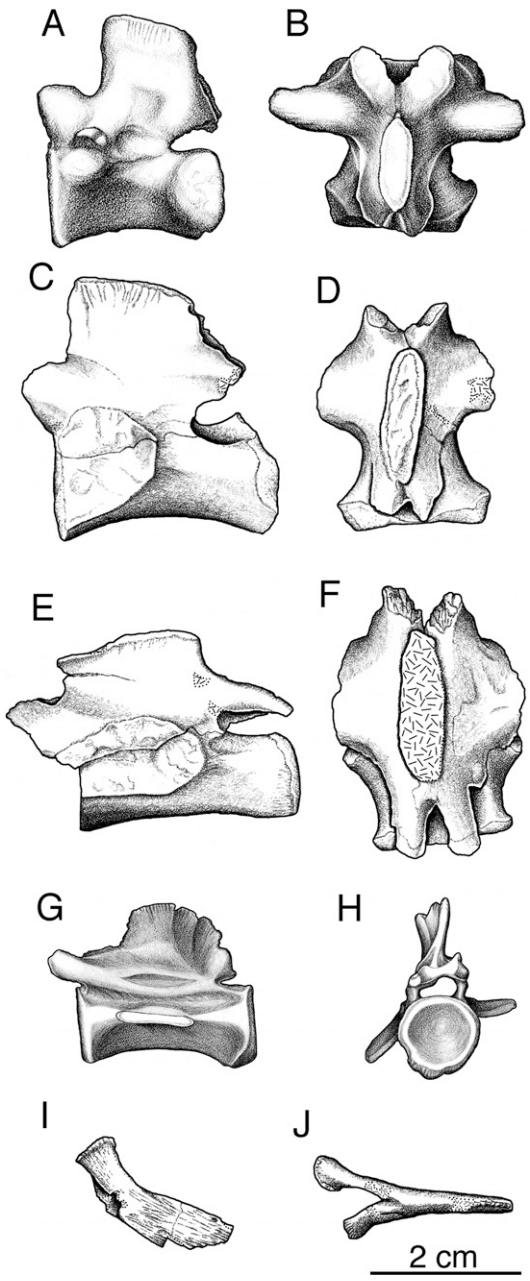


FIGURE 5. Sacral and caudal vertebrae of *Doswellia kaltenbachi* (USNM 244214). **A**, **B**, first sacral vertebra in left lateral (**A**) and dorsal (**B**) views; **C**, **D**, second sacral in left lateral (**C**) and dorsal (**D**) views; **E**, **F**, third sacral in left lateral (**E**) and dorsal (**F**) views; **G**, **H**, distal caudal vertebra in left lateral (**G**) and anterior (**H**) views; **I**, **J**, hemal arch in left lateral (**I**) and ventral (**J**), ventral views

unit with little if any movement between vertebrae. The zygapophyses fit together very closely and those of the second and third sacral vertebra also had interlocking ridges and grooves. The articular surfaces of the postzygapophyses of the third sacral are curved rather than flat. The posterior end of the first sacral centrum, both ends of the second sacral, and the anterior end of the third sacral are acoelous. Furthermore, the large second and third sacral ribs connected across the first and second, and second and third sacrals, respectively (Fig. 5C–F).

**Caudal Vertebrae**—The precise anteroposterior sequence of the thirteen isolated caudal vertebrae is uncertain, but they clearly include elements from the proximal, middle, and distal regions of the tail (Weems, 1980). Five proximal caudals have large ribs that attached to the side of the centrum and neural arch. No diapophyses or parapophyses are present. The distal expansion of the neural spine present in the dorsals and sacrals continues into the proximal caudals, but has largely disappeared by the fifth caudal. The articular facets of the zygapophyses are damaged on most of these proximal caudals. The prezygapophyses of the first caudal are horizontal, but the medial and lateral edges of each are curved dorsally, forming a cup-shaped articular surface that matches the curved surface of the postzygapophysis of the last sacral. The postzygapophyses of the first and second caudal have horizontal and flat articular facets. There is a change in the orientation of the zygapophyses in these proximal caudals from horizontal to medially inclined (Weems, 1980). The outlines of the ends of the centra also change from horizontally oval to circular or vertically oval. Two incomplete vertebrae from the middle region of the tail have large, thin lateral projections that are likely fused ribs. The projection on the posterior of this pair of caudals is bifurcated with the anterior process the larger of the two. As noted by Weems (1980), the first of these two middle caudals has a strongly angled anterior end of the centrum that faces anteroventrally. Whether this indicates a ventral bend in the tail depends on the unknown shape of the centrum of the next anterior caudal. More distal caudals have progressively smaller fused caudal ribs; the neural spines are increasingly blade-like, and the centra are tall and narrow (Fig. 5G, H).

Facets for hemal arches are present on the third proximal caudal and all subsequent preserved vertebrae of the tail. The blade of a hemal arch is thin, expanded distally, and covered by numerous fine ridges that are prominent along the ventral and distal edges (Fig. 5I, J).

**Cervical Ribs**—Each cervical rib has a stout and flattened proximal end with clearly separated capitulum and tuberculum (Fig. 6). The capitular and tubercular articular facets are concave with an elevated rim surrounded by a thicker, roughened rim that is continuous with the surface of the rib. These two rims are likely attachment sites for the inner articular capsule and outer fibrous capsule of the synovial joint between the rib and vertebra. Immediately distal to the articular facets is a constriction followed by an expansion forming the flattened proximal end. The anterior edge of this proximal region is thin and rounded. Distally, the rib continues as a narrow process with a triangular cross-section. The length of this posterior process is greater on the more posterior cervical ribs where it attains a length at least equal to the centrum. When articulated with the vertebra, the process is directed posteriorly and ventrally. The entire lateral edge of the rib from the

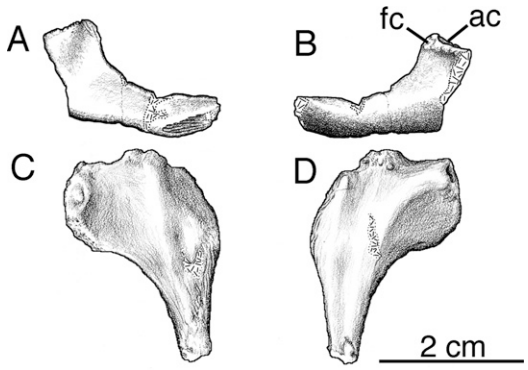


FIGURE 6. Cervical ribs of *Doswellia kaltenbachi* (USNM 214823). **A**, **B**, left axial rib in dorsal (**A**) and ventral (**B**) views; **C**, **D**, fifth cervical rib in dorsal (**C**) and ventral (**D**) views.

proximal expanded region to the tip of the posterior process is flattened, faces laterally, and covered by a series of long ridges and grooves.

**Anterior Dorsal Ribs**—In addition to their greater size, anterior dorsal ribs are distinguishable from cervical ribs by their division into distinctive proximal and distal regions that enclose an angle of between 90° and 120° (Weems, 1980). There is a gradual lateral shift of the facet for the tuberculum from the first to last anterior dorsal rib that is clearly linked with the parallel increase in the length of the diapophysis and the increase in contact between the capitulum and diapophysis. At the corner between the proximal and distal regions, ribs of the second (Fig. 7A, B) and third dorsal vertebra each has a rounded and rugose projection that is directed primarily dorsally, but also laterally and anteriorly. This projection is especially prominent on the third dorsal ribs, but is absent from all subsequent ribs. Instead, the fourth dorsal rib has a highly rugose flange extending dorsolaterally (Fig. 7C, D). This flange is thinner and longer on the fifth anterior dorsal rib (Fig. 7E, F). The length of the distal segment of the ribs increases from the first to last anterior dorsal vertebrae and its cross-sectional shape changes from circular to oval. The sixth anterior dorsal rib is transitional between the anterior and posterior dorsals (Weems, 1980). It has a long capitulum similar in length to that of the posterior dorsal ribs and its dorsal surface is flattened and covered by ridges as on the posterior dorsal ribs. It shares with the anterior dorsal ribs a corner between a proximal and distal segment. The distal segment is truncated with an expanded and deeply cup-shaped terminus. It is uncertain whether this rib was continued by a cartilaginous structure (Weems, 1980) or possibly pathological because the left sixth rib is not preserved. When the anterior dorsal ribs are articulated with their respective vertebrae, the anterior section of the rib cage widens posteriorly, but is overall relatively narrow.

**Posterior Dorsal Ribs**—Regardless of the uncertainty of the true shape of the sixth dorsal rib, there is a sudden change in the outline of the rib cage between the anterior and posterior dorsal vertebrae. Ribs of the posterior dorsal vertebrae project primarily laterally with only a slight curvature distally, thus lacking a distal region (Fig. 7G, H). This shape and the elongated diapophyses of the posterior result in a considerable increase in the width of the rib cage between the sixth and seventh dorsal vertebrae. Maximum width of the rib cage is attained at the first three of the posterior dorsal vertebrae. More posteriorly, there is a gradual decrease in the width. A distinctive feature of each posterior dorsal rib is its flattened, slightly expanded dorsal surface covered by numerous ridges.

**Sacral Ribs**—The preserved portion of the first sacral rib is similar to the last dorsals. Although it presumably articulated with the ilium (Weems, 1980), this cannot be confirmed because only a segment of the right first sacral rib is known. The second sacral rib (Fig. 8A, B) is distinctly different from the first with an enlarged holocephalous contact with the centra of both the first and second sacral vertebrae (Fig. 5A–D). Distally, it expands to form a square-shaped contact with the ilium. There is an additional articular facet along the posterior side of distal expansion. The proximal end of the distinctive third sacral rib (Fig. 8C, D) joins with the centra of the second and third sacrals, but, unlike the second sacral rib, it expands distally into a dorsoventrally flat blade that contacts both the ilium and the posterior facet on the second sacral rib.

**Caudal Ribs**—The first caudal rib has a holocephalous proximal end and a shaft that is triangular in cross-section for most of its length (Fig. 8E, F). The base of this triangular cross-section faces dorsally and, like the posterior dorsal ribs, bears many fine parallel ridges extending from the proximal to the distal end. Its blade-like distal expansion is twisted so that one side faces anterodorsally and the other faces posteroventrally. Ridges cover both sides. Two separate oval articular facets are found at the distal tip. The second caudal rib has an identical morphology to the first though slightly shorter in length. The fourth caudal rib shaft is oval in cross-section proximally and flattened distally (Fig. 8G, H). The distal half also bears many parallel ridges on its dorsal and ventral surfaces. There are no articular facets at the distal tip of the fourth caudal rib. All more posterior caudal ribs are fused to their vertebrae. Each is a dorsoventrally flattened blade extending laterally and becoming smaller in successively posterior caudal vertebrae.

**Gastralia**—Numerous isolated gastralia were found among the skeletal elements of the type material of *Doswellia*. All are long with one expanded rounded end that tapers to a blunt tip (Fig. 8I, J). There is variation in the size of the expanded end.

### Osteoderms

*Doswellia* has an extensive series of articulated osteoderms that extend along the dorsal and lateral sides of the body from the back of the skull to at least the base of the tail. These osteoderms are arranged in a highly regular pattern to form longitudinal and transverse rows. Several osteoderms make up each transverse row. Although their precise relationship with the vertebrae is uncertain, there was probably a single transverse row for each vertebra with the paramedian osteoderms joined over the neural spine, as in many other archosauriform reptiles. There is also evidence of isolated osteoderms possibly associated with the limbs. With the exception of a section of osteoderms from the posterior dorsal region that remain articulated or at least closely associated, most osteoderms are separated from their respective vertebrae and from other elements in their respective transverse row. Thus, in most regions one can only describe the features of those osteoderms from the cervical, anterior dorsal, posterior dorsal, pelvic, and caudal regions, and, in some instances, provide additional information on variation within a transverse row.

The majority of osteoderms of *Doswellia* have a square or rectangular shape. Only those that comprise the "nuchal collar" (Weems, 1980) have a more irregular shape. Few can be described as truly flat; even those from the midline typically have a ventral curvature. The dorsal surface of each osteoderm is covered by deep pits except for the anterior margin that forms an articular facet overlapped by the osteoderm in the next anterior transverse row. An anteromedial projection of the articular facet is found on some osteoderms. A prominent sulcus separates the articular facet from the portion of the osteoderm with pits. A dorsal eminence with numerous small pits is present on nearly every osteoderm. This eminence is oriented anteroposteriorly and typically has a gentle curvature. A few scattered foramina are often present on the ventral surface. The posteroventral margin of each osteoderm has a series of transverse ridges where it overlaps a succeeding osteoderm. Some also have a thickened anteromedial corner on the ventral side covered by a set of parallel ridges. The simple overlap between osteoderms in a longitudinal row implies flexibility between successive rows. Long projections that fit into deep recesses along the medial and, with the exception of the most lateral osteoderm, lateral sides interlocked those osteoderms within a transverse row into a rigid sheet of bone. Hence, each transverse row of osteoderms would flex as a unit against the rows anterior and posterior to it. Those osteoderms along the lateral margin of the osteoderm shield have a curved, slightly jagged lateral edge that lacks pits.

**Cervical Osteoderms**—Two pieces of curved bone (Fig. 9A–D) found associated with the skull are parts of a "nuchal collar" (Weems, 1980). Rather than fragments of a pair of large plates that met along the midline, each is actually composed of several smaller osteoderms. The grooves on the dorsal

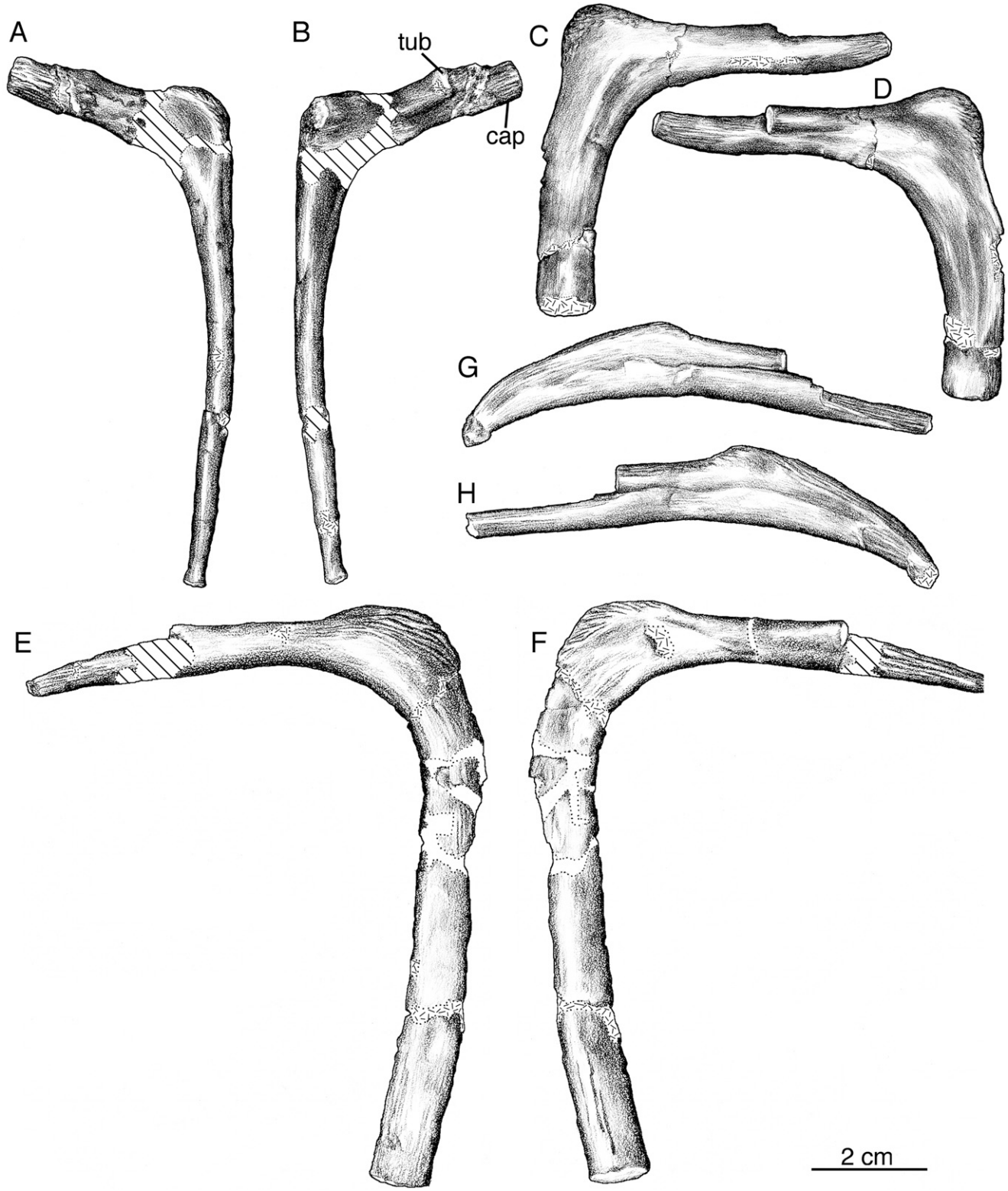


FIGURE 7. Dorsal ribs of *Doswellia kaltenbachi* (USNM 244214). **A**, **B**, left second dorsal rib in anteroventral (**A**) and posterodorsal (**B**) views; **C**, **D**, right fourth dorsal rib in anteroventral (**C**) and posteroventral (**D**) views; **E**, **F**, left fifth dorsal rib in anteroventral (**E**) and posterodorsal (**F**) views; **G**, **H**, right ninth dorsal rib in anterior (**G**) and posterior (**H**) views.

surface, originally interpreted by Weems as evidence for the location of cornified epidermal scales, can be traced onto the ventral surface and are actually sutures between the osteoderms. Further support for this interpretation is the presence of a dorsal eminence on each of the middle three osteoderms in the larger fragment (Fig. 9A) and the partial separation of two of the osteoderms of the smaller fragment revealing interlocking projections (Fig. 9C, D). The direction of the dorsal eminences on

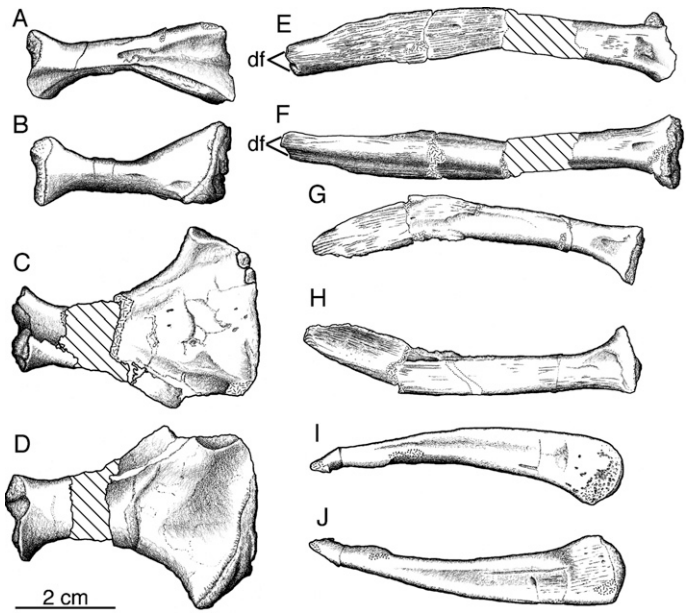


FIGURE 8. *Doswellia kaltenbachi* (USNM 244214). **A**, **B**, left second sacral rib in dorsal (**A**) and ventral (**B**) views; **C**, **D**, right third sacral rib in dorsal (**C**) and ventral (**D**) views; **E**, **F**, right first caudal rib in dorsal (**E**) and ventral (**F**) views; **G**, **H**, right fourth caudal rib in dorsal (**G**) and ventral (**H**) views; **I**, **J**, gastral "rib" in ventral (**I**) and dorsal (**J**) views.

the larger fragment indicates the anterior and posterior margins and the rounded swelling on the ventral side of the larger fragment corresponds most closely to the thickened anteromedial corner on some osteoderms. Thus, as restored by Weems (1980), the anterior margin is upturned and has a series of parallel ridges. The smaller fragment includes a portion of the posterior margin that is similarly upturned with ventral ridges that correspond to the posterior edge of other osteoderms that overlap the osteoderm in the next transverse row. Laterally, this collar extends around the dorsal portion of the side of the neck. Although the midline is not preserved on either fragment, the size of the larger indicates that the width of the collar is at least equal to the width of the skull in the temporal region. It is unlikely that there was an additional osteoderm attached to the collar (Weems, 1980) because the roughened lateral margins of the two pieces resemble the lateral edges of those osteoderms in the most lateral rows of other osteoderms.

Several osteoderms found with the cervical vertebrae include three whose close proximity to each other suggests that they comprised a transverse row (Fig. 9E–J) and a fourth separated from the three may be part of the same row (Fig. 9K, L). At least one more osteoderm would be in this row since all have projections and recesses on their lateral and medial margins. The three osteoderms in a row are distinct suggesting that if one (Fig. 9I, J) is a paramedian, then there were at least four osteoderms on each side of a transverse row in the cervical region. According to this interpretation, one osteoderm (Fig. 9E, F) would be more laterally placed. This osteoderm differs from the others in the row by its greater ventral curvature and greatly thickened anteromedial corner that is covered ventrally by many ridges and deeply incised grooves. This rugose region may be the attachment site for a myoseptal ligament between a cervical rib and osteoderm. The fourth osteoderm in this set is extremely similar to one of the three in a row. Its shape is also a mirror image of this osteoderm, indicating that it is from the opposite side of the row. The dorsal eminence rises only slightly above the pitting and does not extend anteriorly to the sulcus. In several osteoderms, the dorsal eminence is restricted to the posterior half of the osteoderm.

**Anterior Dorsal Osteoderms**—As there is no clear demarcation between the cervical and anterior dorsal regions and most of the osteoderms from these regions are scattered, only those osteoderms clearly associated with the more posterior of the anterior dorsals likely belong to this region. Most of these osteoderms are from the most lateral longitudinal row on the left side. The more posterior members of this row have a rounded lateral edge (Fig. 10A, B) whereas more anteriorly the lateral margin is straight (Fig. 10C, D). The dorsal eminence is more pronounced than in the cervicals and located close to the suture with the next medial row. It also extends further anteriorly to almost reach the sulcus. Weems (1980) estimated a minimum of three longitudinal rows, but this number cannot be confirmed.

**Posterior Dorsal Osteoderms**—The most lateral osteoderms within many of the transverse rows were associated with the ribs and vertebrae (Weems, 1980:pl. 11) in their apparent correct anterior to posterior sequence. The more anterior of these lateral osteoderms (Fig. 10E, F) has a gentle curvature and a large portion lateral to the dorsal eminence. There is a gradual increase in the amount of curvature and a relative decrease in the size of the osteoderm lateral to the dorsal eminence in the more posterior osteoderms (Fig. 10G, H). The dorsal eminence is located at the point of inflection. The increase in curvature evidently continued back to the pelvic region as shown by very strongly curved, more medial osteoderms found with the pelvic girdle and caudal vertebrae that are either from the posterior dorsal or pelvic regions (Fig. 10I, J).

The only articulated set of plates clearly associated with the posterior dorsal vertebrae (Fig. 10K) provides significantly more information on the osteoderms of this region. The longest articulated transverse row consists of eight osteoderms with four on each side of the midline (Weems, 1980). At least one additional longitudinal row would have been present. The dorsal eminence is more pronounced than on the anterior dorsal and cervical osteoderms and located along the midline of the osteoderm with the exception of those in the lateralmost longitudinal row. The length of the osteoderms in a transverse row increases laterally with the greatest increase along the articular facet. The fourth osteoderm from the midline has a stronger curvature than the others in the same transverse row.

**Pelvic and Sacral Osteoderms**—A series of four unusually shaped osteoderms are associated with the right and left ilia (Fig. 11A, B). The lateral edge is not sutured to other osteoderms indicating that they are the most lateral in each transverse row. Unlike other osteoderms of *Doswellia*, the two middle pelvic osteoderms in the series are deeply sutured along their anterior and posterior margins in addition to their medial edge. Each osteoderm is strongly curved forming a narrow space between the lateral and medial portions that apparently would fit along the dorsal edge of the ilium. The dorsal eminence is located along this line of curvature. The anterior osteoderm is sutured to the next posterior one, but the anterior end tapers to a blunt tip with only a roughened ventral surface to indicate contact with the next anterior osteoderm. The last osteoderm in the series, thought by Weems (1980) to be the first caudal osteoderm, has a thinner posterior margin with reduced ridges for sutural contact with the next posterior osteoderm. It is also interesting because it has a medial suture next to the dorsal eminence unlike the other osteoderms. However, it is unlikely that this suggests that the other osteoderms are formed by the fusion of two separate pieces (Weems, 1980) because none shows any evidence of a suture next to the dorsal eminence. A possible transitional osteoderm between the pelvic and caudal series from the opposite side was clearly sutured along

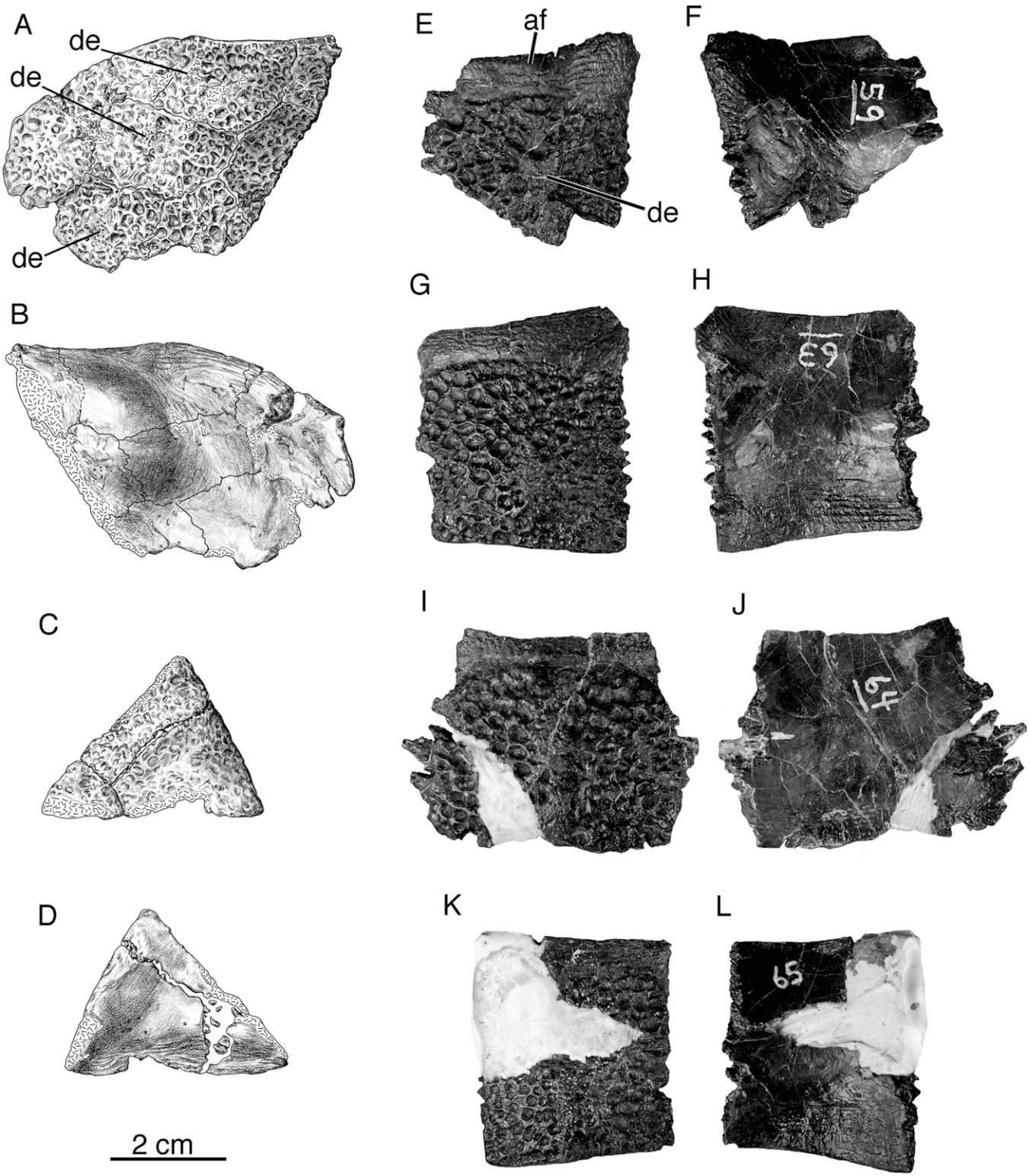


FIGURE 9. Osteoderms of *Doswellia kaltenbachi* (USNM 214823). **A**–**D**, portions of sutured nuchal osteoderms in dorsal (**A**, **B**) and ventral (**C**, **D**) views; **E**–**L**, cervical osteoderms in dorsal (**E**, **G**, **I**, **K**) and ventral (**F**, **H**, **J**, **L**) views.

its anterior and medial borders, but, like most other osteoderms, has a thinner posterior edge with transverse ridges that overlapped the next posterior osteoderm (Fig. 11C, D).

Several mostly fragmentary osteoderms found between the widely separated halves of the pelvic girdle are probably those above the sacral vertebrae (Fig. 11E, F). As described by Weems (1980), the width of each osteoderm is close to or greater than its length.

**Caudal Osteoderms**—Scattered osteoderms associated with the jumbled caudal vertebrae are primarily caudal osteoderms,

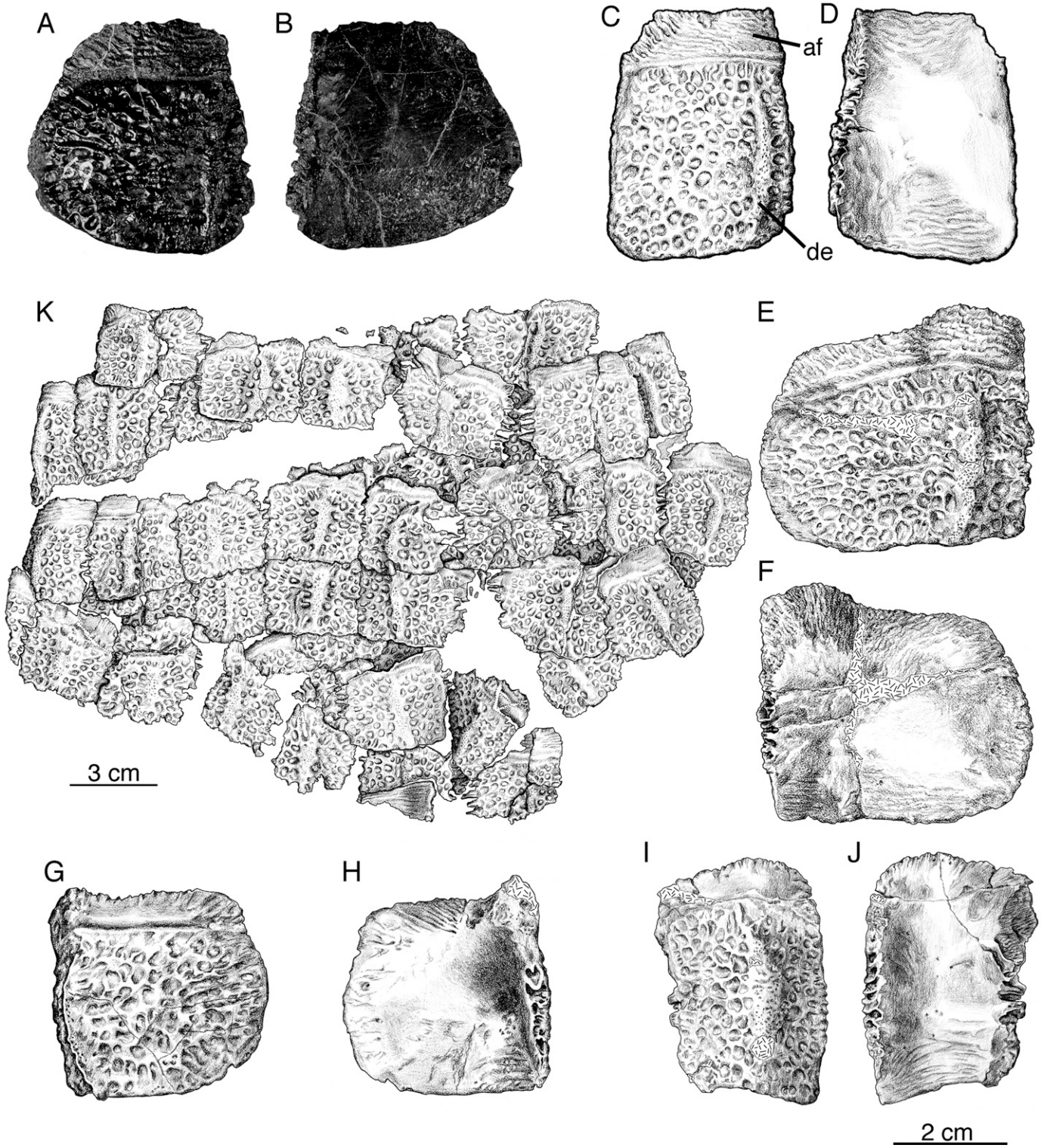


FIGURE 10. Dorsal osteoderms of *Doswellia kaltenbachi* (USNM 244214). **A**–**D**, anterior dorsal osteoderms in dorsal (**A**, **C**) and ventral (**B**, **D**) views; **E**–**J**, posterior dorsal osteoderms in dorsal (**E**, **G**, **I**) and ventral (**F**, **H**, **J**) views; **K**, portion of mostly articulated posterior dorsal osteoderms in dorsal view.

but probably include some from the sacral region. More proximal caudal osteoderms (Fig. 11G, H) have a similar shape to the sacral osteoderms, whereas those found alongside more distal caudal vertebrae have a greater anteroposterior length (Fig. 11I, J). The dorsal eminence remains prominent on the proximal osteoderms, but is absent on one lateral osteoderm (Fig. 11K, L). The latter has the same anteroposterior length as a more medial osteoderm with a dorsal eminence (Fig. 11I, J),

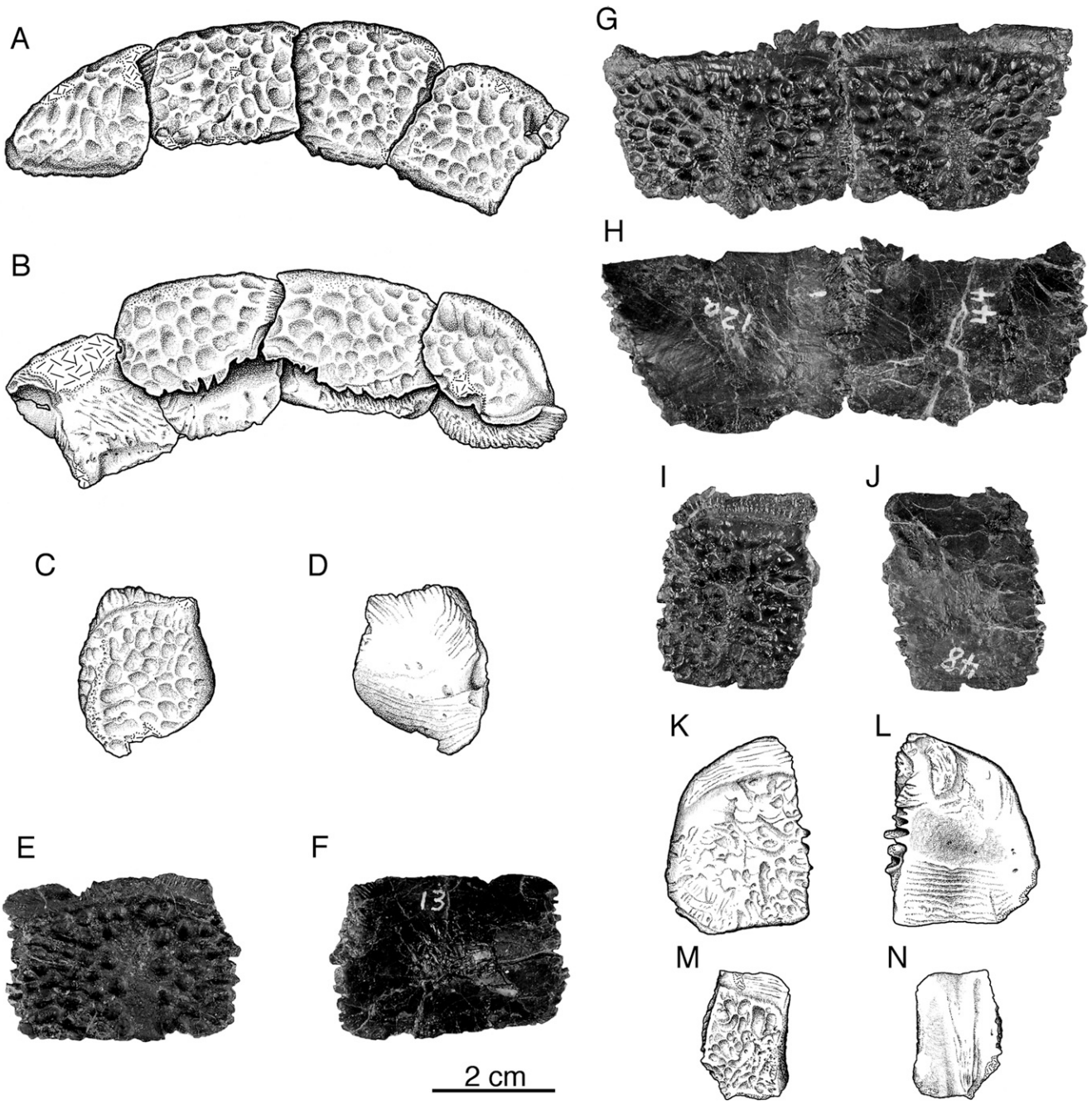


FIGURE 11. Pelvic, sacral, and caudal osteoderms of *Doswellia kaltenbachi* (USNM 244214). **A**, **B**, pelvic osteoderms associated with left ilium in lateral (**A**) and medial (**B**) views; **C**, **D**, probable transitional osteoderm between pelvic and caudal osteoderms in dorsal (**C**) and ventral (**D**) views; **E**, **F**, sacral osteoderm in dorsal (**E**) and ventral (**F**) views; **G**-**N**, caudal osteoderms in dorsal (**G**, **I**, **K**, **M**) and ventral (**H**, **J**, **L**, **N**) views.

indicating that there is a lateral reduction and loss of the dorsal eminence in transverse rows of caudal osteoderms. A smaller, more distal caudal osteoderm located more medially in a transverse row lacks a dorsal eminence, but does have the small pits found on the dorsal eminence (Fig. 11M, N).

**Possible Appendicular Osteoderm**—A small, flat, and thin piece of bone with an irregular shape (Fig. 12) lacks association with any element of the skeleton. It has a few small and scattered pits and a slightly sculptured edge, but has no sutural contacts with another element. It did not overlap nor was it overlapped by another bone. Its shape is similar to that of possible appendicular osteoderms in other archosaurs (Clark et al., 2000; Sues et al., 2003).

## Appendicular Skeleton

**Clavicle**—The slender right clavicle has a dorsal segment attached to the anterior edge of the scapulocoracoid that twists anteriorly and ventrally towards the interclavicle (Fig. 13A–C). Scattered ridges are present on the flattened lateral side of the dorsal segment. Along the ventrolateral surface at the corner between the tall dorsal segment and the smaller, flattened

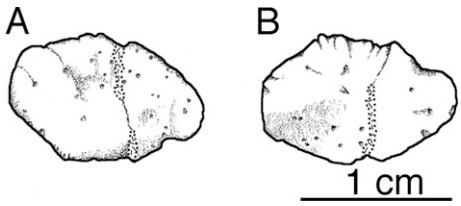


FIGURE 12. *Doswellia kaltenbachi* (USNM 244214). **A**, **B**, possible appendicular osteoderm in dorsal (**A**) and ventral (**B**) views.

ventral segment, there is a thin flange with a rugose margin (Fig. 13A, B).

**Interclavicle**—The cruciform interclavicle (Fig. 13D) has a thin, dorsally concave posterior blade. Anteriorly, a pair of deep recesses for the reception of the clavicles are separated by only a narrow median strip of bone.

**Ilium**—The dorsal blade of the very distinctive ilium (Fig. 14A, B) is deflected laterally so that the plesiomorphically medial side faces dorsally. A portion of the dorsal edge of the iliac blade ends abruptly at a flat surface indicating a continuation in cartilage. Many fine, parallel ridges are present along both sides of the dorsal edge of the iliac blade. An especially well-developed field of ridges extends across two-thirds of the dorsally facing side of the iliac blade from the anterior corner. Ridges on the ventrally facing side of the iliac blade are also largely confined to the anterior two thirds of the dorsal edge. Both sets of ridges are likely attachment sites for the longissimus and iliocostalis muscle groups. A large, oval articular surface for the second sacral rib and a posterior, narrower one for the blade-like third sacral rib are between the iliac blade and acetabular region. The acetabulum has a prominent shelf along its dorsal rim.

**Ischium**—As observed by Weems (1980), a large area of the right ischium has a growth of spongy bone with a roughened, irregular surface that may be the result of a bone infection (Fig. 14C). The left ischium is not preserved. The ischia met along the midventral side of the pelvic girdle. A damaged, posteriorly directed projection on the posterior end of the ischium (Fig. 14C, D) is probably the ischial tuberosity from which Mm. ischiocaudalis and flexor tibialis internus may have arisen (Hutchinson, 2001).

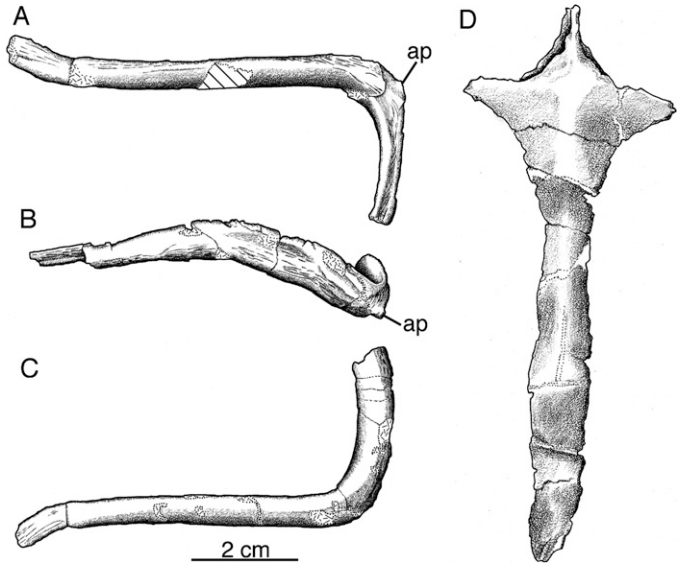


FIGURE 13. Appendicular elements of *Doswellia kaltenbachi* (USNM 244214). **A**–**C**, right clavicle in posterior (**A**), lateral (**B**), and anterior (**C**) views; **D**, interclavicle in ventral view.

**Pubis**—The large, plate-like pubis (Fig. 14E) makes only a small contribution to the acetabulum. The pubic tubercle, the likely attachment point for the ambiens and abdominal oblique muscles (Dilkes, 2000; Hutchinson, 2001) rather than M. rectus abdominis (Weems, 1980), is reduced in size compared to those of other archosauromorphs such as rhynchosaurs and proterosuchids. The obturator foramen is an oval opening just beneath the acetabulum. A circular hole found only on the left pubis is a puncture left by a tooth of a predator or scavenger, most likely a phytosaur (Weems, 1980). The right pubis has a small, rugose area on its lateral side between the obturator foramen and acetabulum suggesting that the probable bone infection on the right ischium had spread to the pubis.

**Femur**—The poorly preserved left femur of USNM 186989 is crushed and many areas of the bone surface are highly fractured or missing (Fig. 15). The original preparation also removed significant regions of the bone surface. The femur has a sigmoidal shape, but there are no visible external features such as a fourth trochanter or scars indicating the attachment of thigh muscles.

## PHYLOGENETIC ANALYSIS

*Doswellia kaltenbachi* has long been a phylogenetic enigma among Triassic diapsid reptiles. While the evidence strongly indicates placement of *Doswellia* among the Archosauria as traditionally conceived (Weems, 1980), support for a more precise placement among the many archosaurian clades has remained elusive. Certain features such as the extensive dermal armor, long, slender snout, and horn-like extensions of the squamosals of *Doswellia* are shared with crocodylomorphs and phytosaurs, but relationships with either group were dismissed by Weems (1980) on the basis of other characters of *Doswellia*, including the plate-like structure of the pelvis with a laterally deflected ilium, absence of ventral keels on the cervical centra, and the greater number of sacral vertebrae. Weems rejected a relationship with aetosaurs (Stagonolepididae) because the osteoderms of *Doswellia* are clearly distinctive in the number of sagittal rows and the absence of any ventral osteoderms although Bonaparte (1982) did classify *Doswellia* with aetosaurs. He was only able to conclude that, at best, the shared presence of elongate snouts, teeth on the pterygoid, and the absence of postfrontals suggested a possible relationship with a lineage of proterosuchids and proterochampsids. Nonetheless, Weems (1980) decided that the best compromise given the incompleteness of the skeletal material, its obvious distinctiveness, and lack of clear evidence of affinities with any established group of archosaurs was to erect a new "thecodontian" suborder solely for the reception of *Doswellia*.

In the only cladistic analysis to include *Doswellia* (Benton and Clark, 1988), a sister group relationship with proterochampsids was hypothesized based upon the shared absence of a postfrontal and a reversal of the shape of the pelvis from three-rayed to massive. Referral to the Proterochampsidae was suggested (Olsen et al., 1989) but later rejected by Long and Murry (1995) who could only conclude that *Doswellia* was likely a very specialized archosauromorph and perhaps not even an archosauriform. More recently, Lehman and Chatterjee (2005) merely referred to *Doswellia* as an archosauriform.

### Methods

A data matrix of 15 taxa and 85 characters was constructed to determine the most likely phylogenetic position of *Doswellia* among archosauriforms. Taxa included two archosauromorph outgroups (*Mesosuchus* and *Prolacerta*) determined by previous analyses to be most closely related to archosauriforms (Dilkes,

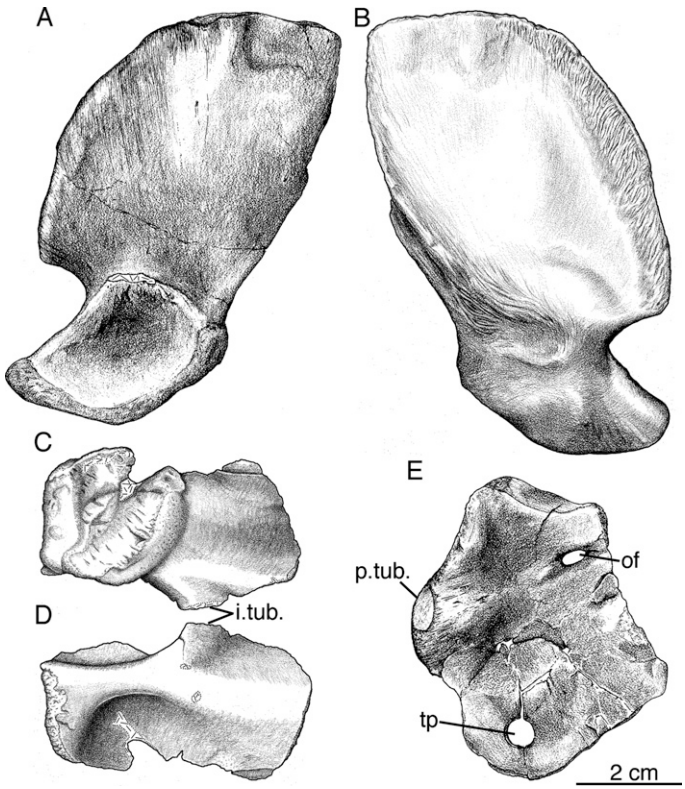


FIGURE 14. Pelvic girdle of *Doswellia kaltenbachi* (USNM 244214). **A**, **B**, left ilium in ventrolateral (**A**) and dorsomedial (**B**) views; **C**, **D**, right ischium in ventral (**C**) and dorsal (**D**) views; **E**, left pubis in ventrolateral view.

1998; Modesto and Sues, 2004) and thirteen ingroup taxa consisting of *Proterosuchus*, *Euparkeria*, *Doswellia*, *Erythrosuchus*, Proterochampsidae, *Parasuchus* ("*Paleorhinus*"), Stagonolepididae, *Gracilisuchus*, *Scleromochlus*, *Marasuchus*, *Turfanosuchus*, *Yonghesuchus*, and *Qianosuchus*. Data for *Proterosuchus*, *Euparkeria*, *Erythrosuchus*, *Paleorhinus*, *Gracilisuchus*, *Scleromochlus*, *Marasuchus*, *Turfanosuchus*, *Yonghesuchus*, and *Qianosuchus* were obtained primarily from the literature (Ewer, 1965; Romer, 1972a; Chatterjee, 1978; Sereno and Arcucci, 1994; Welman, 1998; Benton, 1999; Wu and Russell, 2001; Wu et al., 2001; Gower, 2003; Senter, 2003; Li et al., 2006) and supplemented by personal observations of *Proterosuchus*, *Euparkeria*, and *Gracilisuchus*. The present study is the first to include *Turfanosuchus*, *Yonghesuchus*, and *Qianosuchus* in a single phylogenetic analysis. Proterochampsidae is a composite taxon based upon *Proterochampsa barrionuevoi* (Sill, 1967; personal observation) and *Chanaresuchus bonapartei* (Romer 1971, 1972b; personal observation). Similarly, the scorings for Stagonolepididae are derived from *Stagonolepis* and *Aetosaurus* (Walker, 1961; Gower and Walker, 2002).

The character-taxon matrix was analyzed with PAUP* 4.0b10 (Swofford, 2002). All characters were run unordered and given equal weight, and multistate characters were treated as polymorphisms. The branch-and-bound algorithm was selected to search for the most parsimonious cladograms. DELTRAN character state optimization was chosen. Assessment of the relative support for nodes in the most parsimonious cladograms was determined by bootstrap analysis and Bremer decay analysis (Bremer, 1988). The branch-and-bound option was selected for the bootstrap with 1,000 replicates. Only those groups with >50% frequency were kept. Bremer support was calculated with the program TreeRot (Sorenson, 1999).

**Results**

A single most parsimonious tree was obtained (Fig. 16) with a length of 151 steps. This tree has a consistency index (CI) of 0.5894, homoplasy index (HI) of 0.4172, CI excluding uninformative characters of 0.5811, HI excluding uninformative characters of 0.4189, a retention index (RI) of 0.7033, and a rescaled consistency index (RCI) of 0.4146. The most basal nodes are well supported as shown by bootstrap values larger than 90% and Bremer support numbers of 7 and 9 (Fig. 16). However, both measures of support decrease markedly at those branches with *Erythrosuchus*, *Doswellia*, Proterochampsidae, *Turfanosuchus*, *Yonghesuchus* and the base of Archosauria.

## DISCUSSION

The results of the phylogenetic analysis are largely compatible with those reported in other papers. *Proterosuchus* is positioned as the most basal archosauriform as found in previous phylogenetic studies (Benton and Clark, 1988; Juul, 1994; Bennett, 1996; Benton, 2004). One major difference is the relative positions of *Euparkeria* and *Erythrosuchus*. Previous cladistic studies have consistently placed *Euparkeria* closer to the crown-clade Archosauria than *Erythrosuchus* (Benton, 1985; Gauthier, 1986; Benton and Clark, 1988; Sereno and Arcucci, 1990; Sereno, 1991; Juul, 1994; Bennett, 1996; Benton, 2004) whereas the present analysis reverses this order (Fig. 16). The clade of *Erythrosuchus* and derived archosauriforms excluding *Euparkeria* (node B in Fig. 16) is supported by a bootstrap value of 68% and a Bremer value of 1. Node B is supported by four unambiguous characters:

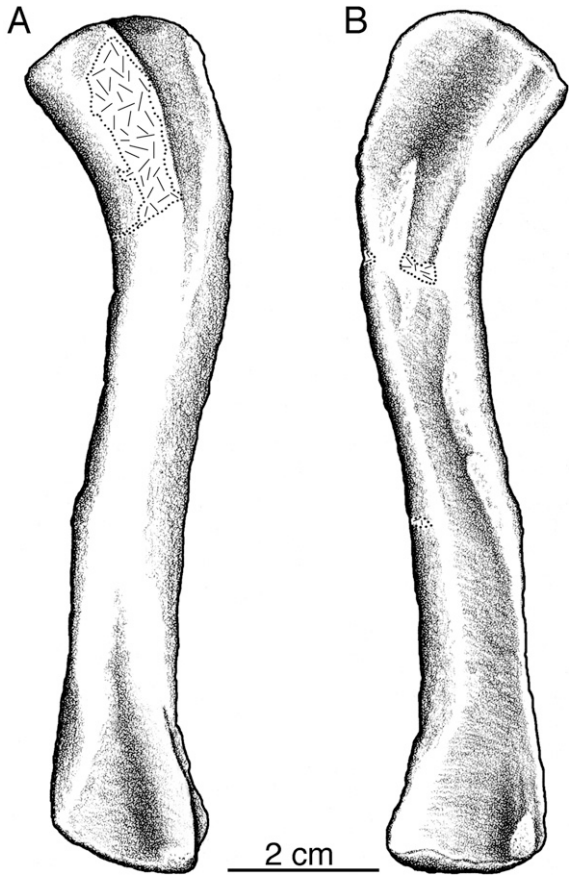


FIGURE 15. Left femur of *Doswellia kaltenbachi* (USNM 186989) in dorsal (**A**) and ventral (**B**) views.

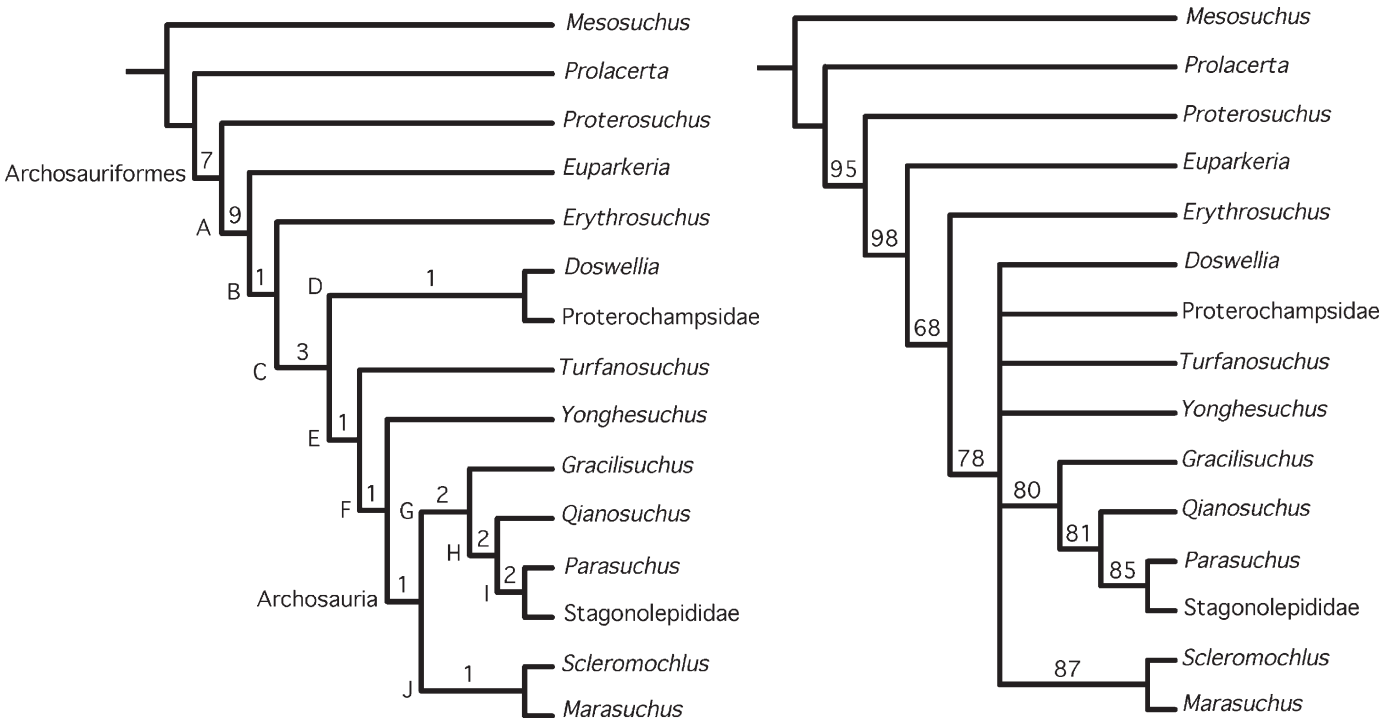


FIGURE 16. Results of phylogenetic analysis. **A**, single most parsimonious cladogram. Numbers are Bremer support values and capital letters refer to nodes listed in Appendix 3; **B**, bootstrap analysis results with support values. All nodes with less than 50% support are collapsed.

a simple vertical or diagonal contact between the premaxilla and maxilla (character 7), a reversal to the absence of an anterior surangular foramen (character 43), mostly dichocephalous trunk ribs (character 52), and a non-bifurcate second sacral rib (character 53).

In many cases, characters that in previous studies have supported a relationship between *Euparkeria*, proterochampsids, and archosaurs excluding *Erythrosuchus* are actually present in erythrosuchids. These characters include the presence of an antorbital fossa (Benton, 1985; Benton and Clark, 1988; Sereno and Arcucci, 1990; Juul, 1994), absence of a parietal foramen (Benton, 1985; Benton and Clark, 1988; Juul, 1994; Bennett, 1996), presence of thecodont dentition (Benton, 1985; Benton and Clark, 1988), ribs all single- or double-headed (Benton, 1985; Benton and Clark, 1988), presence of dorsal body osteoderms (Benton, 1985; Benton and Clark, 1988; Sereno and Arcucci, 1990, Sereno, 1991), a scapula with a length that is more than twice its maximum width (Benton, 1985; 2004), loss of the astragalocalcaneal canal (Sereno and Arcucci, 1990; Sereno, 1991), loss of distal tarsals 1 and 2 (Sereno and Arcucci, 1990; Sereno, 1991), and a pedal digit IV that is significantly shorter than pedal digit III (Sereno and Arcucci, 1990; Sereno, 1991; Bennett, 1996). *Erythrosuchus* has an antorbital fenestra, teeth that are distinctly thecodont, two-headed ribs, dorsal osteoderms, a tall scapula with a length greater than twice the maximum width, and a pedal digit IV that is shorter than pedal digit III (Smith and Swart, 2002; Gower, 2003). Furthermore, *Erythrosuchus* probably lacks a parietal foramen (Gower, 2003), which is also absent in *Proterosuchus* (Welman, 1998), and lacks an astragalocalcaneal canal and distal tarsals 1 and 2 (Gower, 2003).

Several other characters used to exclude *Erythrosuchus* from a clade of *Euparkeria*, proterochampsids, and archosaurs are problematic because they cannot be scored for *Erythrosuchus* either due to the incompleteness of specimens or the character lacks a clear definition. These characters include a well-developed otic notch (Benton, 1985; Benton and Clark, 1988), an interclavicle with reduced, tab-like lateral processes (Sereno, 1991), presence of "archosaur humerus" (Bennett, 1996), ulna much stouter than radius (Bennett, 1996), asymmetry of manus with digits I and II stouter than digits IV and V which are reduced and divergent, and digit III is longest (Bennett, 1996), pelvis markedly three-rayed (Benton, 1985), strongly downturned pubic tuber (Benton, 2004), hindlimbs placed under body (also referred to as a semi-erect or erect posture) (Benton, 1985; Benton and Clark, 1988; Bennett, 1996), femur with markedly sigmoidal curvature (Sereno and Arcucci, 1990; Sereno, 1991; Bennett, 1996), and significant rotation between astragalus and calcaneum (Benton, 1985; Benton and Clark, 1988) that was incorporated in the character of a crocodyloid tarsus by Bennett (1996). The interclavicle is unknown for *Erythrosuchus* and the manus is incomplete in the available specimens (Gower, 2003). No clear, consistent features of an "archosaur humerus" have been defined, and distal condyles of the humerus that are less ventrally directed (Bennett, 1996) appear to be true for *Erythrosuchus* (Gower, 2003). A measure of the relative stoutness of the ulna and radius is lacking (Bennett, 1996), thus this character is difficult to score for *Erythrosuchus*. A pelvic girdle with three rays and a strongly downturned pubic tuber differs from the broad, plate-like pelvis of more plesiomorphic archosauromorphs such as *Mesosuchus* and *Prolacerta* (Dilkes, 1998). However, the pelvis of *Erythrosuchus* is actually more similar to that of *Euparkeria* than to that of *Prolacerta* (Ewer, 1965; Gower, 2003). Posture of the hindlimbs is difficult to assess, as there exists a continuum between sprawling and erect postures. *Erythrosuchus* was likely intermediate between sprawling and erect postures though perhaps closer to erect depending upon amount of femoral rotation during locomotion (Kubo and Benton, 2007). The degree of sigmoidal curvature of the femur is difficult to measure even without the complication of distortion by crushing. The curvature of femora of basal archosauromorphs such as *Mesosuchus* and *Prolacerta* is very similar to that of femora in more derived taxa such as *Euparkeria* (Ewer, 1965; Dilkes,

1998). *Erythrosuchus* has a femur with some curvature, more so than present in the femur of *Proterosuchus* (Gower, 2003). Lastly, a complex articulation between the astragalus and calcaneum that allows rotational movement may not be present in *Euparkeria* that may share mesotarsal ankle structure with *Erythrosuchus* (Gower, 1996).

*Doswellia* is the sister taxon of Proterochampsidae united by the unambiguous characters of the absence of the postfrontal and a reversal to the plesiomorphic structure of an ischium with a small posteroventral process. Absence of the postfrontal has been proposed previously as a shared derived feature of *Doswellia* and proterochampsids (Benton and Clark, 1988). This node of the cladogram is supported by a Bremer value of 1, but collapses in the bootstrap cladogram.

One other important result of the present analysis is the poor support for Archosauria as measured by bootstrap and Bremer decay analysis (Fig. 16). Only two characters, viz. absence of teeth on the pterygoid and a gentle posteroventral curvature of the cervical ribs, support Archosauria as opposed to six characters listed in the most recent phylogenetic review of archosaurs (Benton, 2004). These six characters are: 1) absence of teeth on palatine and vomer, 2) manual digit IV with four or fewer phalanges, 3) ventral astragalocalcaneal articular facet larger than the dorsal articulation, 4) calcaneal tuber oriented more than 45° posterolaterally, 5) articular surfaces for fibula and distal tarsal 4 on calcaneum are continuous, and 6) articular facet for metatarsal V on distal tarsal 4 is less than half of the lateral surface of distal tarsal 4. The critical distinction is the addition of *Turfanosuchus*, *Yonghesuchus*, and *Qianosuchus* to the present study that have shown the previously proposed synapomorphies either have a more inclusive distribution or have equivocal assignments. Teeth are absent from the palatine of *Turfanosuchus*, absent from both the palatine and vomer of *Qianosuchus*, and unknown for the vomer of *Turfanosuchus* and the vomer and palatine of *Yonghesuchus* (Wu and Russell, 2001; Wu et al., 2001; Li et al., 2006). Absence of teeth on the vomer and palatine (designated as separate characters in the present study) is equivocal and no longer supports Archosauria. However, teeth remain on the palatal ramus of the pterygoid in *Turfanosuchus* and *Yonghesuchus* (Wu and Russell, 2001; Wu et al., 2001), and demonstrate that the absence of at least one region of palatal teeth remains a viable archosaurian synapomorphy. The number of phalanges on manual digit IV is a character of uncertain utility because it cannot be scored for the majority of taxa in the present study. The relative size of the ventral astragalocalcaneal articular facet is unknown for *Turfanosuchus* and *Yonghesuchus* (Wu and Russell, 2001; Wu et al., 2001), and may diagnose a more inclusive clade than Archosauria. Posterolateral orientation of the calcaneal tuber and continuous articular surfaces on the calcaneum for the fibula and distal tarsal 4 are present in *Turfanosuchus* and unknown in *Yonghesuchus*, and diagnosis Node E of the cladogram (Fig. 16). The relative size of the articular facet for metatarsal V on distal tarsal 4 is unknown for *Turfanosuchus* and *Yonghesuchus*, and would have an equivocal distribution on the cladogram.

The relative positions of *Parasuchus* and *Gracilisuchus* (Fig. 16) differ from previous studies (e.g. Benton and Clark, 1988; Sereno, 1991; Parrish, 1993; Juul, 1994) where phytosaurs are placed near the base of Crurotarsi, below *Gracilisuchus*, stagonolepidids, crocodylomorphs, and the various "rauisuchian" taxa. In this study, *Gracilisuchus* is at the base of Crurotarsi whereas *Parasuchus* is placed as the sister taxon to Stagonolepididae above *Qianosuchus*. Node H (*Qianosuchus*, *Parasuchus*, and Stagonolepididae) is diagnosed by the absence of a shelf/ridge along the dorsal margin of the antorbital fossa that extends across the lacrimal, prefrontal, frontal portion of orbit, and postorbital (character 16), a more vertical orientation of the basisphenoid (character 28), and a robust, pendent fibular cranial trochanter (character 67). *Parasuchus* and Stagonolepididae (node I) are separated from *Qianosuchus* by the synapomorphies of an entrance of the anterior end of the jugal into the antorbital fenestra (character 14) and a carapace of dermal osteoderms on the ventral side of the body (character 85). Support for this arrangement is relatively strong with a Bremer value of 2 for nodes H and I and bootstrap values of 81% and 85% for nodes H and I, respectively.

In summary, *Doswellia* is an archosauriform reptile closely related to but not part of Archosauria. It is the sister taxon to Proterochampsidae as proposed previously (Benton and Clark, 1988). This relationship and the placements of *Turfanosuchus* and *Yonghesuchus* are not as strongly supported as other nodes due to the incomplete material presently available for these taxa. Nonetheless, the data do support the hypotheses that *Qianosuchus* is a crurotarsan archosaur and *Turfanosuchus* and *Yonghesuchus* are not archosaurs. The hypothesized relationship between *Doswellia* and Proterochampsidae is of paleobiogeographic interest. The traversodont cynodont *Boreogomphodon* from correlative strata in the neighboring (and originally connected) Richmond basin of the Newark Supergroup in Virginia is most closely related to basal traversodont taxa from southern Africa and Brazil (Sues and Olsen, 1990; Sues and Hopson, unpublished data). Thus, *Doswellia* would represent an additional "Gondwanan" element in the faunal assemblage from the Richmond and Taylorsville basins.

## ACKNOWLEDGMENTS

The authors wish to thank Michael Brett-Surman, Robert Purdy, and Jann Thompson (Department of Paleobiology, National Museum of Natural History) for the loan of the holotype and paratype. Thanks are also extended to Diane Scott (Dept. of Biology, University of Toronto at Mississauga) for preparation and illustration of the cranial remains; her work was supported by an operating grant from the Natural Sciences and Engineering Research Council of Canada to H-DS. For their assistance with illustrations, we thank Richard Mulcare for Figure 14A, E; Kevin Dupuis for Figures 4, 6C, 6D, 7, 9A–D, 10C–J, 13D, and 14B; and Elsie Chung for Figure 5A, B, G, H.

## LITERATURE CITED

Bennett, S. C. 1996. The phylogenetic position of the Pterosauria within the Archosauromorpha. Zoological Journal of the Linnean Society 118:261–308.

Benton, M. J. 1985. Classification and phylogeny of the diapsid reptiles. Zoological Journal of the Linnean Society 84:97–164.

Benton, M. J. 1999. *Scleromochlus taylori* and the origin of dinosaurs and pterosaurs. Philosophical Transactions of the Royal Society of London, B 354:1423–1426.

Benton, M. J. 2004. Origin and relationships of Dinosauria; pp. 7–19 in D. B. Weishampel, P. Dodson, and H. Osmólska (eds.), The Dinosauria. 2nd ed. Berkeley, California: University of California Press.

Benton, M. J., and J. M. Clark. 1988. Archosaur phylogeny and the relationships of the Crocodylia; pp. 295–338 in M. J. Benton (ed.), The Phylogeny and Classification of the Tetrapods, Volume 1: Amphibians, Reptiles, Birds. Oxford, England: Clarendon Press.

Bonaparte, J. F. 1982. Classification of the Thecodontia. Geobios, Mémoire Spécial 6:99–112.

Bremer, K. 1988. The limits of amino-acid sequence data in angiosperm phylogenetic reconstruction. Evolution 42:795–803.

Case, E. C. 1928. Indications of a cotylosaur and of a new form of fish from the Triassic beds of Texas, with remarks on the Shinarump Conglomerate. Contributions from the Museum of Paleontology, University of Michigan 3:1–14.

Chatterjee, S. 1978. A primitive parasuchid (phytosaur) reptile from the Upper Triassic Maleri Formation of India. Palaeontology 21:83–127.

Clark, J. M., H.-D. Sues, and D. S Berman. 2000. A new specimen of *Hesperosuchus agilis* from the Upper Triassic of New Mexico and

the interrelationships of basal crocodylomorph archosaurs. Journal of Vertebrate Paleontology 20:683–704.
Cornet, B., and P. E. Olsen. 1990. Early to Middle Carnian (Triassic) flora and fauna of the Richmond and Taylorsville basins, Virginia and Maryland, U.S.A. Virginia Museum of Natural History, Guidebook 1:1–83.
Cruickshank, A. R. I. 1972. The proterosuchian thecodonts; pp. 89–119 in K. A. Joysey and T. S. Kemp (eds.), Studies in Vertebrate Evolution. Edinburgh, Scotland: Oliver and Boyd.
Dilkes, D. W. 1998. The Early Triassic rhynchosaur *Mesosuchus browni* and the interrelationships of basal archosauromorph reptiles. Philosophical Transactions of the Royal Society of London, B 353:501–541.
Dilkes, D. W. 2000. Appendicular myology of the hadrosaurian dinosaur *Maiasaura peeblesorum* from the Late Cretaceous (Campanian) of Montana. Transactions of the Royal Society of Edinburgh: Earth Sciences 90:87–125.
Evans, S. E. 1986. The braincase of *Prolacerta broomi* (Reptilia; Triassic). Neues Jahrbuch für Geologie und Paläontologie, Abhandlungen 173:181–200.
Ewer, R. F. 1965. The anatomy of the thecodont reptile *Euparkeria capensis* Broom. Philosophical Transactions of the Royal Society of London, B 248:379–445.
Frey, E. 1988. Anatomie des Körperstammes von *Alligator mississippiensis* Daudin. Stuttgarter Beiträge zur Naturkunde, Serie A 424:1–106.
Gauthier, J. 1986. Saurischian monophyly and the origin of birds. Memoirs of the California Academy of Sciences 8:1–55.
Gower, D. J. 1996. The tarsus of erythrosuchid archosaurs, and implications for early diapsid phylogeny. Zoological Journal of the Linnean Society 116:347–375.
Gower, D. J. 1997. The braincase of the early archosaurian reptile *Erythrosuchus africanus*. Journal of Zoology (London) 242:557–576.
Gower, D. J. 2003. Osteology of the early archosaurian reptile *Erythrosuchus africanus* Broom. Annals of the South African Museum 110:1–84.
Gower, D. J., and A. G. Sennikov. 1996. Morphology and phylogenetic informativeness of early archosaur braincases. Palaeontology 39:883–906.
Gower, D. J., and A. G. Sennikov. 1997. *Sarmatosuchus* and the early history of the Archosauria. Journal of Vertebrate Paleontology 17:60–73.
Gower, D. J., and E. Weber. 1998. The braincase of *Euparkeria*, and the evolutionary relationships of birds and crocodilians. Biological Reviews 73:367–411.
Gower, D. J., and A. D. Walker. 2002. New data on the braincase of the aetosaurian archosaur (Reptilia: Diapsida) *Stagonolepis robertsoni* Agassiz. Zoological Journal of the Linnean Society 136:7–23.
Gregory, J. T. 1945. Osteology and relationships of *Trilophosaurus*. University of Texas Special Publication 4401:273–359.
Heckert, A. B., and S. G. Lucas. 1999. A new aetosaur (Reptilia: Archosauria) from the Upper Triassic of Texas and the phylogeny of aetosaurs. Journal of Vertebrate Paleontology 19:50–68.
Heckert, A. B., S. G. Lucas, L. F. Rinehart, J. A. Spielmann, A. P. Hunt, and R. Kahle. 2006. Revision of the archosauromorph reptile *Trilophosaurus*, with a description of the first skull of *Trilophosaurus jacobsi*, from the Upper Triassic Chinle Group, West Texas, USA. Palaeontology 49:621–640.
Huber, P., S. G. Lucas, and A. P. Hunt. 1993. Vertebrate biochronology of the Newark Supergroup Triassic, eastern North America. New Mexico Museum of Natural History & Science Bulletin 3:179–186.
Huene, F. von 1946. Die grossen Stämme der Tetrapoden in den geologischen Zeiten. Biologisches Zentralblatt 65:268–275.
Hutchinson, J. R. 2001. The evolution of pelvic osteology and soft tissues on the line to extant birds (Neornithes). Zoological Journal of the Linnean Society 131:123–168.
Juul, L. 1994. The phylogeny of basal archosaurs. Palaeontologia Africana 31:1–38.
Kubo, T., and M. J. Benton. 2007. Evolution of hindlimb posture in archosaurs: limb stresses in extinct vertebrates. Palaeontology 50:1519–1529.
Lehman, T., and S. Chatterjee. 2005. Depositional setting and vertebrate biostratigraphy of the Triassic Dockum Group of Texas. Journal of Earth System Science 114:325–351.
LeTourneau, P. 2003. Tectonic and climatic controls on the stratigraphic architecture of the Late Triassic Taylorsville basin, Virginia and Maryland; pp. 12–58 in P. LeTourneau and P. E. Olsen (eds.), The Great Rift Valleys of Pangea in Eastern North America. Volume Two: Sedimentology, Stratigraphy, and Paleontology. New York, NY: Columbia University Press.
Li, C., X.-c. Wu, Y.-n. Cheng, T. Sato, and L. Wang. 2006. An unusual archosaurian from the marine Triassic of China. Naturwissenschaften 93:200–206.
Long, R. A., and P. A. Murry. 1995. Late Triassic (Carnian and Norian) tetrapods from the southwestern United States. New Mexico Museum of Natural History & Science Bulletin 4:1–254.
Lucas, S. G., and P. Huber. 2003. Vertebrate biostratigraphy and biochronology of the nonmarine Late Triassic; pp. 143–191 in P. LeTourneau and P. E. Olsen (eds.), The Great Rift Valleys of Pangea in Eastern North America. Volume Two: Sedimentology, Stratigraphy, and Paleontology. New York, NY: Columbia University Press.
Modesto, S. P., and H.-D. Sues. 2004. The skull of the Early Triassic archosauromorph reptile *Prolacerta broomi* and its phylogenetic significance. Zoological Journal of the Linnean Society 140:335–351.
Mueller, B. D., and W. G. Parker. 2006. A new species of *Trilophosaurus* (Diapsida: Archosauromorpha) from the Sonsela Member (Chinle Formation) of Petrified Forest National Park, Arizona; pp. 119–125 in W. G. Parker, S. R. Ash, and R. B. Irmis (eds.), A Century of Research at Petrified Forest National Park 1906–2006: Geology and Paleontology. Museum of Northern Arizona Bulletin 62.
Olsen, P. E., R. W. Schlische, and P. J. W. Gore. (eds.) 1989. Tectonic, Depositional, and Paleoecological History of Early Mesozoic Rift Basins, Eastern North America. 28th International Geological Congress. Field Trip Guidebook T351. American Geophysical Union, Washington, DC, 174 pp.
Osborn, H. F. 1903. The reptilian subclasses Diapsida and Synapsida and the early history of the Diaptosauria. Memoirs of the American Museum of Natural History 1:449–507.
Parrish, J. M. 1993. Phylogeny of the Crocodylotarsi, with reference to archosaurian and crurotarsan monophyly. Journal of Vertebrate Paleontology 13:287–308.
Romer, A. S. 1971. The Chañares (Argentina) Triassic reptile fauna. XI. Two new long-snouted thecodonts, *Chanaresuchus* and *Gualosuchus*. Breviora 379:1–22.
Romer, A. S. 1972a. The Chañares (Argentina) Triassic reptile fauna. XIII. An early ornithosuchid pseudosuchian, *Gracilisuchus stipanicorum*, gen. et sp. nov. Breviora 389:1–24.
Romer, A. S. 1972b. The Chañares (Argentina) Triassic reptile fauna. XII. The postcranial skeleton of the thecodont *Chanaresuchus*. Breviora 385:1–21.
Senter, P. 2003. New information on cranial and dental features of the Triassic archosauriform reptile *Euparkeria capensis*. Palaeontology 46:613–621.
Sereno, P. C. 1991. Basal archosaurs: phylogenetic relationships and functional implications. Society of Vertebrate Paleontology Memoir 2 11:1–53.
Sereno, P. C., and A. B. Arcucci. 1990. The monophyly of crurotarsal archosaurs and the origin of bird and crocodile ankle joints. Neues Jahrbuch für Geologie und Paläontologie, Abhandlungen 180:21–52.
Sereno, P. C., and A. B. Arcucci. 1994. Dinosaurian precursors from the Middle Triassic of Argentina: *Marasuchus lilloensis*, gen. nov. Journal of Vertebrate Paleontology 14:53–73.
Sill, W. D. 1967. *Proterochampsa barrionuevoi* and the early evolution of the Crocodilia. Bulletin of the Museum of Comparative Zoology, Harvard University 135:415–446.
Smith, R. M. H., and R. Swart. 2002. Changing fluvial environments and vertebrate taphonomy in response to climatic drying in a Mid-Triassic rift valley fill: the Omingonde Formation (Karoo Supergroup) of central Namibia. Palaios 17:249–267.
Sorenson, M. D. 1999. TreeRot, version 2. Boston, Massachusetts: Boston University.
Sues, H.-D. 2003. An unusual new archosauromorph reptile from the Upper Triassic Wolfville Formation of Nova Scotia. Canadian Journal of Earth Sciences 40:635–649.
Sues, H.-D., and P.E. Olsen. 1990. Triassic vertebrates of Gondwanan aspect from the Richmond basin of Virginia. Science 249:1020–1023.
Sues, H.-D., P. E. Olsen, J. G. Carter, and D. M. Scott. 2003. A new crocodylomorph archosaur from the Upper Triassic of North Carolina. Journal of Vertebrate Paleontology 23:329–343.

Swofford, D. L. 2002. PAUP* Phylogenetic Analysis Using Parsimony (*and other methods). 4.0b10. Sunderland, Massachusetts: Sinauer Associates.

Walker, A. D. 1961. Triassic reptiles from the Elgin area: *Stagonolepis*, *Dasygnathus* and their allies. Philosophical Transactions of the Royal Society of London, B 244:103–204.

Weems, R. E. 1980. An unusual newly discovered archosaur from the Upper Triassic of Virginia, U.S.A. Transactions of the American Philosophical Society 70:1–53.

Welman, J. 1998. The taxonomy of the South African proterosuchids (Reptilia, Archosauromorpha). Journal of Vertebrate Paleontology 18:340–347.

Wu, X.-C., and A. P. Russell. 2001. Redescription of *Turfanosuchus dabanensis* (Archosauriformes) and new information on its phylogenetic relationships. Journal of Vertebrate Paleontology 21:40–50.

Wu, X.-C., J. Liu, and J.-L. Li. 2001. The anatomy of the first archosauriform (Diapsida) from the terrestrial Upper Triassic of China. Vertebrata PalAsiatica 39:251–265.

Submitted January 15, 2008; accepted July 08, 2008.

APPENDIX 1. Description of characters used in phylogenetic analysis. The bracketed number (0, 1, or 2) refers to the character state listed for the character.

1. Lower temporal (infratemporal) fenestra: present and open ventrally (0); present and closed ventrally (1); absent (2) (Dilkes, 1998).
2. Antorbital fossa, depressed regions on maxilla and lacrimal forming a definite inset margin to the antorbital fenestra: absent (0); present (1) (Benton, 2004).
3. Antorbital fenestra: absent (0); present (1) (Dilkes, 1998).
4. Shape of premaxilla: downturned ventral margin (0); horizontal ventral margin (1) (modified from Dilkes, 1998).
5. External nares location: close to midline and near tip of rostrum (0); marginal and near tip of rostrum (1); close to midline and posteriorly situated (2) (modified from Dilkes, 1998).
6. Lacrimal: contacts nasal, but does not reach external naris (0); does not contact nasal or reach naris (1) (modified from Dilkes, 1998).
7. Form of suture between premaxilla and maxilla above dentigerous margin: notch present in maxilla (0); simple vertical or diagonal contact (1) (modified from Dilkes, 1998).
8. Location of nasolacrimal canal foramen/ina: in lacrimal (0); between lacrimal and prefrontal (1) (Senter, 2003).
9. Ratio of lengths of nasal and frontal: $\leq$1.0 (0); $>$1.0 (1) (Dilkes, 1998).
10. Postfrontal: present (0); absent (1) (modified from Benton, 2004).
11. Parietal foramen: present (0); absent (1) (Dilkes, 1998).
12. Postparietals: present and fused (0); absent (1) (modified from Juul, 1994).
13. Supratemporal: present (0); absent (1) (Dilkes, 1998).
14. Anterior end of jugal: enters into antorbital fenestra (0); excluded by the contact of the maxilla and lacrimal (1) (Clark et al., 2000).
15. Squamosal overhanging quadrate and quadratojugal laterally: absent (0); present (1) (modified from Benton, 2004).
16. Dorsal margin of antorbital fossa is a shelf/ridge that extends across lacrimal, prefrontal, frontal portion of orbital rim, and postorbital: absent (0); present (1) (new character).
17. Depression on descending process of postorbital: absent (0); present (1) (Wu et al., 2001).
18. Quadratojugal: present without an anterior process (0); present with an anterior process that contacts jugal (1) (modified from Dilkes, 1998).
19. Contact between ectopterygoid and maxilla: absent (0); present (1) (Dilkes, 1998).
20. Orientation of basipterygoid processes: anterolateral (0); lateral (1) (Dilkes, 1998).
21. Position on basisphenoid of foramina of cerebral branches of internal carotid arteries leading to the pituitary fossa: posterior/posteroventral (0); lateral (1) (Parrish, 1993).
22. Exoccipitals and opisthotics: discrete (0); fused (1) (Juul, 1994).
23. Number of foramina for hypoglossal nerve: two (0); one (1) (Gower and Sennikov, 1996).
24. Anteroventral process of prootic below trigeminal foramen: lateral ridge present (0); lateral ridge absent (1) (Gower and Sennikov, 1996).
25. Position of external abducens foramen on prootic: ventral (0); anterior (1) surface (Benton, 2004).
26. Laterosphenoid: absent (0); present (1) (Dilkes, 1998).
27. Position of occipital condyle: anterior to craniomandibular joint (0); even with craniomandibular joint (1); posterior to craniomandibular joint (2) (modified from Dilkes, 1998).
28. Orientation of basisphenoid: horizontal (0); more vertical (1) (Gower and Sennikov, 1996).
29. Parabasisphenoid plate between cristae ventrolaterales: intertuberal plate present (0); absent (1) (Gower and Sennikov, 1996).
30. Semilunar depression on parabasisphenoid: present (0); absent (1) (Gower and Sennikov, 1996).
31. Association between paroccipital process and parietal: no contact (0); contact present immediately lateral to supraoccipital (1) (modified from Dilkes, 1998).
32. Medial margin of exoccipitals: no contact (0); contact to exclude basioccipital from floor of braincase (1) (Gower and Sennikov, 1996).
33. Anterior and posterior edges of marginal teeth: serrations absent (0); serrations present (1) (Dilkes, 1998).
34. Curvature of marginal teeth: absent (0); present (1) (Dilkes, 1998).
35. Cross-sectional shape of marginal teeth: oval (0); laterally compressed (1) (Dilkes, 1998).
36. Posterior extent of mandibular and maxillary tooth rows: subequal (0); unequal with the maxillary tooth extending further posteriorly (1) (Bennett, 1996).
37. Vomerine teeth: present (0); absent (1) (Dilkes, 1998).
38. Palatine teeth: present (0); absent (1) (Dilkes, 1998).
39. Teeth on palatal ramus of pterygoid: present (0); absent (1) (modified from Dilkes, 1998).
40. Teeth on transverse flange of pterygoid: single row (0); absent (1) (modified from Dilkes, 1998).
41. Pterygoids: join anteriorly (0); remain separate (1) (Dilkes, 1998).
42. Lateral mandibular fenestra: absent (0); present (1) (Dilkes, 1998).
43. Anterior surangular foramen: absent (0); present (1) (Modesto and Sues, 2004).
44. Posterior surangular foramen: absent (0); present (1) (Modesto and Sues, 2004).
45. Postaxial cervical intercentra: present (0); absent (1) (Dilkes, 1998).
46. Dorsal vertebrae intercentra: present (0); absent (1) (Dilkes, 1998).
47. Ratio of lengths of centra of mid-cervical and mid-dorsal vertebrae: $\leq$1.0 (0); $>$1.0 (1) (modified from Dilkes, 1998).
48. Neural arches of mid-dorsals: deep excavation (0); no excavation or shallow excavation (1) (modified from Dilkes, 1998).
49. Distal ends of cervical neural spines: no expansion (0); expansion present in form of a flat table (1) (Dilkes, 1998).
50. Distal ends of dorsal neural spines: no expansion (0); expansion present in form of a flat table (1) (modified from Dilkes, 1998).
51. Cervical ribs: sharp angle between heads and shaft such that rib lies close to cervical vertebrae (0); gentle curvature of shaft in a posteroventral direction (1) (New character).
52. Trunk ribs: mostly holocephalous (0); mostly dichocephalous (1) (Dilkes, 1998).
53. Second sacral rib: bifurcated (0); not bifurcated (1) (modified from Dilkes, 1998).
54. Interclavicle lateral processes: elongate, making interclavicle T-shaped (0); reduced (1) (Benton, 2004).
55. Anterior margin of interclavicle: notch present between articular facets for clavicles (0); narrow and bluntly pointed separation between articular facets for clavicles (1) (modified from Dilkes, 1998)
56. Posterior stem of interclavicle: little change in width along entire length (0); expansion present (1) (Dilkes, 1998).
57. Scapulocoracoid notch at anterior junction of scapula and coracoid: absent (0); present (1) (Benton, 2004).
58. Shape of scapular blade: tall and rectangular with height/maximum width of base $\leq$2.0 (0); tall and narrow with height/maximum width of base $>$2.0 (1) (modified from Bennett, 1996 and Dilkes, 1998).
59. Forelimb-hindlimb length ratio: $>$ 0.55 (0); $<$ 0.55 (1) (Benton, 2004).
60. Dorsal margin of ilium: convex with broadly rounded anterior and posterior ends (0); straight or with only a portion slightly convex and bluntly pointed anterior and posterior ends (1) (modified from Dilkes, 1998).
61. Preacetabular process on iliac blade: absent (0); present (1) (Benton, 2004).
62. Pubic tubercle: prominent (0); reduced to rugosity (1) (Hutchinson, 2001).

63. Ischium caudoventral process: small and ischium shorter than iliac blade (0); large and ischium longer than the iliac blade (1) (Benton, 2004).
64. Fourth trochanter of femur: absent (0); present (1) (modified from Juul, 1994).
65. Intertrochanteric fossa on ventral aspect of proximal portion of femur: present (0); absent (1) (Benton, 2004).
66. Tibia-femur ratio: <1.0 (0); ≥1.0 (1) (Benton, 2004).
67. Fibular cranial trochanter (insertion site for iliofibularis muscle): low rugosity (0); robust pendent trochanter (1) (Benton, 2004).
68. Astragalocalcaneal canal: present (0); absent (1) (Bennett, 1996).
69. Crural facets on astragalus: separated by a non-articular surface (0); continuous (1) (Sereno, 1991).
70. Orientation of calcaneal tuber: lateral (0); deflected more than 45° posterolaterally (1) (Sereno, 1991).
71. Articular surfaces for fibula and distal tarsal IV on calcaneum: separated by a non-articular surface (0); continuous (1) (Sereno, 1991).
72. Hemicylindrical calcaneal condyle for articulation with fibula: absent (0); present (1) (Parrish, 1993).
73. Astragalar tibial facet: concave (0); saddle-shaped (1) (Sereno, 1991).
74. Calcaneal tuber shaft proportions: taller than broad (0); broader than tall (1) (Sereno, 1991).
75. Calcaneal tuber distal end: anteroposteriorly compressed (0); rounded (1) (Sereno, 1991).
76. Ventral astragalocalcaneal articular facet: small (0); larger (1) than dorsal articulation (Sereno, 1991).
77. Centrale: present (0); absent (1) (Benton, 2004).
78. First and second distal tarsals: present (0); absent (1) (modified from Dilkes, 1998).
79. Metatarsus configuration: metatarsals diverging from ankle (0); compact metatarsus with metatarsals I-IV tightly bunched (1) (Benton, 2004).
80. Metatarsal II-IV length: less than (0); greater (1) than 50% of tibial length (Benton, 2004).
81. Ratio of lengths of pedal digits III and IV: ≤1.0 (0); >1.0 (1) (Sereno and Arcucci, 1990).
82. Phalanges/phalanx on pedal digit V: present (0); absent (1) (Juul, 1994).
83. Ratio of lengths of pedal digits V and I: >1.0 (0); <1.0 (1) (Juul, 1994).
84. Dorsal body osteoderms: absent (0); present in one or more rows (1) (modified from Bennett, 1996).
85. Dermal osteoderms on ventral side of body: absent (0); articulate and form a carapace (1) (modified from Heckert and Lucas, 1999).

APPENDIX 2. Character-taxon matrix used for phylogenetic analysis.

| | 1 | 2 | 3 | 4 | 5 | 6 | 7 | 8 |
|---|---|---|---|---|---|---|---|---|
| | 0 | 0 | 0 | 0 | 0 | 0 | 0 | 0 |
| *Prolacerta* | 0000000010 | A10?000000 | 0000000000 | 0001110000 | 1011101010 | 0000000000 | 0000000000 | 0000000000 |
| *Mesosuchus* | 0000010000 | 010?000000 | 000??00010 | 0000000001 | 0000101000 | 0000010000 | 0000000000 | 0000000000 |
| *Proterosuchus* | 1010000010 | 1000000101 | 00?0010000 | 1?111110000 | 1111002010 | 0000000001 | 0000000000 | 0000000000 |
| *Euparkeria* | 1111000110 | 1010000111 | 0101110110 | 0011110001 | 1111000011 | 0001000101 | 1111100110 | 0000001100 | 10010 |
| *Doswellia* | 2?????????1 | 111?0??100 | 0111??1011 | 10?10??201 | ?000110111 | 0110112???0 | 1000?????? | ?????????? | ???10 |
| *Erythrosuchus* | 1111101?10 | 1011000111 | 0111110100 | 1111112111 | 1101000000 | 011??20101 | 1110000110 | 0000001100 | 10?10 |
| Proterochampsidae | 1111011?11 | 1110011101 | 0111?10011 | 1011112001 | 1100110100 | 1111?20101 | 1101100110 | 0000001100 | 11110 |
| *Parasuchus* | 1111201110 | 1110101101 | 1101110111 | 0111111111 | 0100110101 | 1111111101 | 1111101111 | 1111111100 | 10011 |
| Stagonolepididae | 1111101110 | 1110000120 | 1101?12111 | 0?10101111 | 0100110??? | 1?111111101 | 1111101?11 | 1111111100 | 10111 |
| *Gracilisuchus* | 1111101?10 | 1011111111 | ??????101? | 0?1111??11 | 0100110100 | 1?1???1101 | 1?10100111 | 1111111100 | ?1110 |
| *Scleromochlus* | 1111102??0 | ???10????0 | ??????20?? | ?????0??11 | 1100110??? | 1?1??20111 | 1121110?21 | ??000?1111 | 01?00 |
| *Turfanosuchus* | 1111101?10 | 1??1011101 | 01011?0011 | ??1112?101 | ?100??2111 | ?21???2??1 | 1121??2111 | 1100??2??? | ????? |
| *Yonghesuchus* | 1111??0?2? | ???1?11?2? | 1???1????? | ??111???01 | ?100?????? | 0?????????? | ?????????? | ?????????? | ????? |
| *Marasuchus* | ?112?????? | ?????????0 | 1101?1?011 | ?????????? | ???2111100 | ?112???111 | 1111110111 | 1000?1111 | 11?0? |
| *Qianosuchus* | 1111101?10 | 1?11001?? | 0????1?11? | ??111??111 | ?1??111?00 | 1??1??10?1 | 1111?01?11 | 1111111100 | ???10 |

Polymorphism of 0&1 is represented by the letter A.

APPENDIX 3. List of unambiguous characters supporting nodes of the most parsimonious cladogram. A letter corresponding to the letters in Fig. 16 represents unnamed clades. A negative sign indicates a reversal in the evolution of the character state.

Archosauriformes: 1, 3, -12, 18, 20, 26, 33, 42, -45, 60.
Node A: 2, 4, 13, 22, 24, 25, 54, 58, 61, 62, 63, 68, 69, 77, 78, 84.
Node B: 7, -43, 52, 53.
Node C: 16, 17, 30, -44, 45, 46, 48, 82.
Node D: 10, -63.
Node E: 70, 71.
Node F: 21.
Archosauria: 39, 51.
Node G: -41, 57, 73, 74, 75.
Node H: -16, 28, 67.
Node I: -14, 85.
Node J: -20, 59, 66, 79, 80, -84.